ORNL/TM-5224

Iterative Solution of the Diffusion and P_1 Finite Element Equations

E. T. Tomlinson
J. C. Robinson
D. R. Vondy

OAK RIDGE NATIONAL LABORATORY
OPERATED BY UNION CARBIDE CORPORATION FOR THE ENERGY RESEARCH AND DEVELOPMENT ADMINISTRATION

DISCLAIMER

Printed in the United States of America. Available from
National Technical Information Service
U.S. Department of Commerce
5285 Port Royal Road, Springfield, Virginia 22161
Price: Printed Copy $6.50; Microfiche $2.25

ORNL/TM-5224
UC-79d - LMFBR Physics

Contract No. W-7405-eng-26

Neutron Physics Division

ITERATIVE SOLUTION OF THE DIFFUSION AND P_1 FINITE ELEMENT EQUATIONS†

E. T. Tomlinson*
J. C. Robinson**
D. R. Vondy

†Submitted to the University of Tennessee by E. T. Tomlinson as a doctoral dissertation in the Department of Nuclear Engineering.

*Computer Sciences Division, Union Carbide Corporation, Nuclear Division.
**Consultant, University of Tennessee, Knoxville, Tennessee.

FEBRUARY 1976

OAK RIDGE NATIONAL LABORATORY
Oak Ridge, Tennessee 37830
operated by
UNION CARBIDE CORPORATION
for the
ENERGY RESEARCH AND DEVELOPMENT ADMINISTRATION

THIS PAGE

WAS INTENTIONALLY

LEFT BLANK

PREFACE AND ACKNOWLEDGMENTS

This report describes work performed by E. T. Tomlinson in partial fulfillment of the requirements for a doctoral degree in the Nuclear Engineering Department of The University of Tennessee under the direction of his major professor, Dr. J. C. Robinson, and a staff member of ORNL's Neutron Physics Division, Dr. D. R. Vondy. Support for the work was provided in the form of a research assistantship through the Neutron Physics Division by ERDA's Liquid Metal Fast Breeder Reactor Program.

The authors wish to express appreciation to the many persons who gave helpful assistance throughout this study. In particular, thanks is offered to Dr. R. A. Lillie and Dr. G. F. Flanagan, both of the ORNL Neutron Physics Division, for their invaluable advice during the various stages of the research. Special thanks are also due to Mrs. Juanita Rye, who typed the report.

THIS PAGE

WAS INTENTIONALLY

LEFT BLANK

ABSTRACT

The purpose of this work is to develop a method for obtaining solutions to the time-independent Boltzmann neutron transport equation on triangular grids with nonorthogonal boundaries and anisotropic scattering. A functional is developed from the canonical form of the multigroup transport equation. The angular variable is then removed by expanding the functional in spherical harmonics retaining only the first two moments and limiting the anisotropic scattering to be linear. The finite element method is then implemented using quadratic Lagrange-type interpolating polynomials to span the spatial domain.

The resultant set of coupled linear equations is then solved iteratively. The applicability of convergence acceleration techniques developed for the finite difference method are tested and implemented where appropriate.

Finally, a number of numerical experiments are performed to evaluate the performance of the proposed method. The results are compared to results obtained by various established methods. In all cases, agreement is excellent.

THIS PAGE

WAS INTENTIONALLY

LEFT BLANK

TABLE OF CONTENTS

LIST OF TABLES

THIS PAGE

WAS INTENTIONALLY

LEFT BLANK

LIST OF FIGURES

CHAPTER I

INTRODUCTION

The objective of this dissertation is to develop a numerical technique for obtaining approximate solutions to the multigroup P_1 equations. Emphasis is placed on the ability of the method to accommodate nonorthogonal boundaries, triangular meshs, and linearly anisotropic scattering. The impetus for choosing these objectives is discussed in the remaining sections of this chapter.

I. Reactor Physics Calculations

Numerical methods for obtaining solutions to neutron transport problems have been widely used and have been shown to be more powerful and versatile than analytic methods. This is particularly true for advanced core designs in which the reactor's geometry and nuclear cross sections are extremely complex. The most widely used numerical method is the finite difference method. This method is quite simple, but suffers from a few important restrictions. Finite difference techniques require small mesh spacing and therefore a relatively large number of unknowns are necessary to adequately describe the behavior of the neutron flux across the solution domain. This manifests itself in the fact that most finite difference computer codes, both those based on the diffusion approximation and the various transport approximations, are limited to two-dimensional calculations.

There are a few coarse mesh three-dimensional computer codes based on the diffusion approximation.[1,2]

The finite difference method has at least one further restriction. The implementation of the difference equations for mesh grids other than regular orthogonal coordinate systems is relatively complex. There are, however, a few computer codes than can perform calculations on triangular and hexagonal grids.[1,2,3] This is of particular importance since current engineering designs for fast breeder reactors are based on arrays of hexagonal subassemblies.

In addition to these geometric complications, there are further calculational difficulties introduced by the nuclear cross sections. It has been shown, that for large fast reactors, the inclusion of only the isotropic component of the scattering cross section results in errors in the calculation of k_{eff} and certain ex-core reaction rates.[4] For a one-dimensional model of the Fast Test Reactor, the use of classic P_0 diffusion theory introduced errors of approximately 2.0 percent in k_{eff} when compared to a S_8P_3 discrete ordinates transport calculation. These errors were reduced to approximately 0.3 percent when the linearly anisotropic component of the scattering cross section was considered in the calculation. These results indicate that higher order scattering must be considered in a calculation if high order accuracy is required.

High order transport methods could be employed to remedy the scattering problem, however, the number of unknowns per spatial node increases rapidly with higher order approximations. This, in

conjunction with the number of nodes necessary to describe the spatial variation of the neutron flux, makes many calculations intractable even on modern computers.

II. The Finite Element Method

Recently, the finite element method has been demonstrated to provide a high accuracy, coarse mesh method for obtaining solutions to the neutron diffusion equation.[5,6] The finite element method was originally developed in the area of structural analysis and has almost totally replaced the finite difference method in that area.[7] The popularity of this method can be attributed to its ability to be applied to almost any geometric configuration and the ease with which higher order approximation procedures can be implemented.

The basis of the finite element method is to partition the solution domain into a number of subdomains or "finite elements." A piecewise continuous polynomial in each of the independent variables is used to approximate the behavior of the unknown functions and its derivatives within each element. The coefficients of these interpolating polynomials are determined by evaluating the unknown function at specified points or nodes within each element. The coupling between elements is realized by requiring the unknown function to be single valued at nodes that are common to two or more adjacent elements. This also insures continuity of the function across the element boundaries. Unlike the synthesis method, the finite element method does not require a prior knowledge of the unknown functions behavior.

The finite element method is generally based on an integral formulation rather than a differential formulation like the finite difference method. This integral formulation can be obtained through a number of techniques. The two basic methods are the weighted residual method and the variational method.(7)

The weighted residual method consists of substituting the interpolating polynomials into the differential equation of interest. Since the interpolating polynomials only approximate the behavior of the unknown function there results a residual. A number of independent weight functions are then chosen. The number of weight functions required is equal to the number of unknown nodal values. The integral of the product of the residual and each weight function is then set to zero. This produces the set of algebraic equations to be solved. The weighted residual method can be subdivided into more specific classes depending on the weight function employed. If a Dirac delta function is used as a weight function, the method is referred to as a collocation method, if the interpolating polynomial is used, the method is referred to as the Galerken method, and if the algebraic equations are obtained by differentiation of the square of the residuals with respect to the unknowns it is referred to as the least squares method.

The variational method is the most widely used method. This method consists of substituting the approximation for the unknown function into a functional whose Euler equation is the differential equation of interest. The first variation of the functional with respect to the nodal unknowns is set equal to zero yielding a set

of coupled algebraic equations. This approach guarantees that the resulting coefficient matrix will be symmetric. This is an important property to consider for numerical computations where computer core storage requirements are important.

III. Applications in Reactor Physics

It is only recently that finite element methods have been investigated for use in the area of reactor physics calculations. Kang and Hansen[8] have applied the method to static neutron diffusion problems, neutron slowing-down problems, and point kinetics problems. Their study was limited to the consideration of rectangular elements in which Hermite polynomials were used as interpolating functions.

Another choice of interpolating functions are the Lagrange polynomials. These polynomials are defined in terms of unknowns on the boundaries and on the interior of each element, thus preventing the imposition of derivative continuity across the element boundaries. The Hermite polynomials are defined in terms of function and its derivative values along the boundaries of each element and therefore derivative continuity can be imposed, but these polynomials become difficult to generate for triangular elements. Semenza et al[9] have used linear Lagrange polynomials with triangular elements and bilinear polynomials with rectangular elements to obtain solutions to the variational form of the multigroup diffusion equations. The results of their calculations for a two-dimensional slab reactor with a planar control rod demonstrate the flexibility of the finite element method to

describe the problem efficiently by allowing many elements to be used near the control rod where steep flux gradients would be expected to appear and relatively few elements in the remainder of the problem.

The multigroup diffusion equations have also been investigated by Kaper et al.[6,10] using higher order Lagrange polynomials. Their work indicated that higher order approximations could lead to substantial computational savings compared to low order finite difference methods. They also concluded that quadratic polynomials are probably the optimum based on the increased number of unknowns needed for higher order approximations versus the increased accuracy obtained by using higher order polynomials.

A number of efforts have been made to apply the finite element method to the neutron transport problem in which both the spatial and angular domains must be considered. Miller et al.[11,12] have applied the method to obtain solutions to the self adjoint, second-order form of the transport equation using the variational method. They used both rectangular and triangular elements in the spatial domain and rectangular, "phase-space," elements in the angular domain. They included linearly anisotropic scattering in their one-dimensional studies, but considered only isotropic scattering in their two-dimensional studies because of the increased complexity.

Kaper et al.[13] have compiled the most significant body of work on the application of the finite element method to neutron transport calculations. Their work contains a study of four different classes of finite element approximations based on: (1) a piecewise polynomial basis in the angular domain, (2) a bi-cubic spline basis

in the angular domain, (3) a surface harmonic approximation in the angular domain, and (4) cubature formulae. The spatial domain is spanned by piecewise continuous Lagrange interpolating polynomials on triangular elements. As in Miller's work, this study was limited to isotropic scattering.

Recently, Lillie[14] has developed a method that accommodates anisotropic scattering and anisotropic neutron flux. The method is based on a variational form of the canonical discrete ordinates equations and employs linear Lagrange interpolating polynomials over triangular elements. The method performs well, but with significant increases in computational time as the order of anisotropy increases.

At present, the only production oriented approach was investigated by Reed et al.[15] and is incorporated into the computer code TRIPLET.[15] This code solves the multigroup discrete ordinates form of the transport equation in triangular geometry. The angular flux is approximated by a Lagrange polynomial over each element. A weighted residual approach is used to generate the necessary algebraic equations. This set of equations is then solved iteratively rather than directly which is the traditional method employed in the finite element method.

The iterative process for solving the finite element equations has also been investigated by Yuan et al.[16] They applied various iterative techniques to the one group, second-order form of the transport equation. Included in their study were the point and block overrelaxation techniques and accelerated block overrelaxation

techniques. They concluded that iterative methods for finite element calculations are as efficient as iterative methods for discrete ordinates calculations.

IV. Scope and Organization

As stated earlier, the objective of this work is to develop a technique for obtaining approximate numerical solutions to the multigroup P_1 equations with particular emphasis on nonorthogonal boundaries, triangular meshes, and linearly anisotropic scattering. To attain these objectives, triangular finite elements are used to span the spatial domain. The neutron flux is allowed to vary quadraticaly over each element. The set of algebraic equations to be solved are obtained through a variational formulation of the P_1 equations. The resultant set of algebraic equations is then solved iteratively.

The development of the mathematical and finite element models are presented in Chapter II. Chapter III presents the development of the numerical techniques employed in this work. The results of a few numerical experiments are presented in Chapter IV. The results of a fixed source problem calculation are compared to a discrete ordinates calculation. A comparison with diffusion theory on a thermal reactor calculation is discussed in this chapter. A comparison with transport theory is also included on a fast reactor calculation to demonstrate the ability of the method to accommodate linearly anisotropic scattering. Chapter V presents the conclusions and a number of recommendations for future efforts.

CHAPTER II

DEVELOPMENT OF THE THEORETICAL MODEL

The derivation of the canonical P_1 equations is presented in the first section of this chapter. The second section contains the development of the finite element equations.

I. The Mathematical Model

The transport of neutrons in a medium can be described by the Boltzmann neutron transport equation. The time independent form of this equation in cartesean coordinates is

$$\vec{\Omega}\cdot\vec{\nabla}\phi(X,Y,E,\vec{\Omega}) + \Sigma(X,Y,E)\ \phi(X,Y,E,\vec{\Omega}) =$$

$$\int_{E'}\int_{\vec{\Omega}'} \Sigma_s(X,Y,E',\vec{\Omega}' \rightarrow E,\vec{\Omega})\ \phi(X,Y,E',\vec{\Omega}')\ d\vec{\Omega}'dE' +$$

$$\frac{f(E)}{4\pi}\int_{E'}\int_{\vec{\Omega}'} \nu\Sigma_f(X,Y,E')\ \phi(X,Y,E',\vec{\Omega}')\ d\vec{\Omega}'dE' +$$

$$Q(X,Y,E,\vec{\Omega}), \qquad (2.1)$$

where

X,Y = position variables,

E = the particle's kinetic energy

$\vec{\Omega}$ = a unit vector which describes the particle's direction of motion,

$\phi(X,Y,E,\vec{\Omega})$ = the time independent angular flux,

$Q(X,Y,E,\vec{\Omega})$ = the source of particles emitted per unit volume and time at position X, Y in direction $\vec{\Omega}$ with energy E,

$\Sigma(X,Y;E'\vec{\Omega}'\rightarrow E,\vec{\Omega})$ = the scattering cross section which describes the probability that a particle with an initial energy E' and direction $\vec{\Omega}'$ undergoes a scattering collision at position X,Y which places it into a direction $\vec{\Omega}$ with energy E,

$\vec{\Omega}\cdot\vec{\nabla}\phi(X,Y,E,\vec{\Omega})$ = the net convective loss per unit volume and time at position X,Y with direction $\vec{\Omega}$ and energy E,

$\nu\Sigma_f(X,Y,E)$ = the neutron production cross section at position X,Y for particles with energy E,

$f(E)$ = the fraction of the total number of particles produced with energy E, and

$\Sigma(X,Y,E)$ = the total cross section at position X,Y for particles with energy E.

The multigroup form of Equation (2.1) is

$$\vec{\Omega}\cdot\vec{\nabla}\ \phi_g(\vec{\Omega}) + \Sigma_g\ \phi_g(\vec{\Omega}) = \sum_{g'=1}^{G} \int_{\vec{\Omega}'} \sum_s^{g'\rightarrow g}(\vec{\Omega}'\cdot\vec{\Omega})\ \phi_{g'}(\vec{\Omega}')\ d\vec{\Omega}' +$$

$$\frac{f_g}{4\pi} \sum_{g'=1}^{G} \nu\Sigma_{fg'} \int_{\vec{\Omega}'} \phi_{g'}(\vec{\Omega}')\ d\vec{\Omega}' + Q_g(\vec{\Omega}), \qquad (2.2)$$

where g = 1, . . ., G and G is the total number of energy groups. The definitions of the variables appearing in Equation (2.2) are

standard and can be found elsewhere.[17] The X,Y variables have also been removed from the equation for simplicity.

If the possibility that a neutron can gain energy through a scattering interaction is neglected, the scattering source term can be simplified to

$$\sum_{g'=1}^{G} \int_{\vec{\Omega}'} \Sigma_s^{g'\to g}(\vec{\Omega}'\cdot\vec{\Omega})\ \phi_{g'}(\vec{\Omega}')\ d\vec{\Omega}' =$$

$$\int_{\vec{\Omega}} \Sigma_s^{g\to g}(\vec{\Omega}'\cdot\vec{\Omega})\ \phi_g(\vec{\Omega}')\ d\vec{\Omega}' + \sum_{g'=1}^{g-1} \int_{\vec{\Omega}'} \Sigma_s^{g'\to g}(\vec{\Omega}'\cdot\vec{\Omega})\ \phi(\vec{\Omega}')\ d\vec{\Omega}'. \qquad (2.3)$$

Rewriting Equation (2.2) for the g^{th} energy group gives

$$\vec{\Omega}\cdot\vec{\nabla}\ \phi_g(\vec{\Omega}) + \Sigma_g\phi_g(\vec{\Omega}) = \int_{\vec{\Omega}'} \Sigma_s^{g\to g}(\vec{\Omega}'\cdot\vec{\Omega})\ \phi_g(\vec{\Omega}')\ d\vec{\Omega}' + S_g(\vec{\Omega}), \qquad (2.4)$$

where

$$S_g(\vec{\Omega}) = \sum_{g'=1}^{g-1} \int_{\vec{\Omega}'} \Sigma_s^{g'\to g}(\vec{\Omega}'\cdot\vec{\Omega})\ \phi_{g'}(\vec{\Omega}')\ d\vec{\Omega}' +$$

$$\frac{f_g}{4\pi} \sum_{g'=1}^{G} \nu\Sigma_{fg'} \int_{\vec{\Omega}'} \phi_{g'}(\vec{\Omega}')\ d\vec{\Omega}' + Q_g(\vec{\Omega}). \qquad (2.5)$$

For further simplification, the subscript g is now dropped and the monoenergetic form of the Boltzmann equation is considered.

The Canonical Transport Equation

Consider Equation (2.4) for $\vec{\Omega}$ and for $-\vec{\Omega}$. For $\vec{\Omega}$ the result is

$$\vec{\Omega}\cdot\vec{\nabla}\ \phi(\vec{\Omega}) + \Sigma\ \phi(\vec{\Omega}) = \int_{\vec{\Omega}'} \Sigma_s(\vec{\Omega}'\cdot\vec{\Omega})\ \phi(\vec{\Omega}')\ d\vec{\Omega}' + S(\vec{\Omega}) \qquad (2.6a)$$

and for $-\vec{\Omega}$

$$-\vec{\Omega}\cdot\vec{\nabla}\,\phi(-\vec{\Omega}) + \Sigma\,\phi(-\vec{\Omega}) = \int_{\vec{\Omega}'} \Sigma_s(\vec{\Omega}'\cdot-\vec{\Omega})\,\phi(\vec{\Omega}')\,d\vec{\Omega}' + S(-\vec{\Omega}). \qquad (2.6b)$$

Decompose the flux, $\phi(\vec{\Omega})$, into its even-parity component, $\psi(\vec{\Omega})$, and its odd-parity component, $\chi(\vec{\Omega})$, as follows

$$\phi(\vec{\Omega}) = \psi(\vec{\Omega}) + \chi(\vec{\Omega}) \qquad (2.7)$$

where

$$\psi(\vec{\Omega}) = \frac{1}{2}[\phi(\vec{\Omega}) + \phi(-\vec{\Omega})], \qquad (2.8)$$

and

$$\chi(\vec{\Omega}) = \frac{1}{2}[\phi(\vec{\Omega}) - \phi(-\vec{\Omega})]. \qquad (2.9)$$

The following definitions are made

$$\Sigma_s^e(\vec{\Omega}'\cdot\vec{\Omega}) = \frac{1}{2}[\Sigma_s(\vec{\Omega}'\cdot\vec{\Omega}) + \Sigma_s(\vec{\Omega}'\cdot-\vec{\Omega})] \qquad (2.10)$$

$$\Sigma_s^o(\vec{\Omega}'\cdot\vec{\Omega}) = \frac{1}{2}[\Sigma_s(\vec{\Omega}'\cdot\vec{\Omega}) - \Sigma_s(\vec{\Omega}'\cdot-\vec{\Omega})] \qquad (2.11)$$

$$S^e(\vec{\Omega}) = \frac{1}{2}[S(\vec{\Omega}) + S(-\vec{\Omega})] \qquad (2.12)$$

$$S^o(\vec{\Omega}) = \frac{1}{2}[S(\vec{\Omega}) - S(-\vec{\Omega})] \qquad (2.13)$$

where these quantities are the even-parity scattering cross section, the odd-parity scattering cross section, the even-parity source and the odd-parity source respectively.

The addition of Equations (2.6) and noting that

$$\int_{\vec{\Omega}'} \Sigma_s^e(\vec{\Omega}'\cdot\vec{\Omega})\,\chi(\vec{\Omega}')\,d\vec{\Omega}' = \int_{\vec{\Omega}'} \Sigma_s^o(\vec{\Omega}'\cdot\vec{\Omega})\,\psi(\vec{\Omega}')\,d\vec{\Omega}' = 0 \qquad (2.14)$$

yields

$$\vec{\Omega}\cdot\vec{\nabla}\,\chi(\vec{\Omega}) + \Sigma\psi(\vec{\Omega}) = \int_{\vec{\Omega}'} \Sigma_s^e(\vec{\Omega}'\cdot\vec{\Omega})\,\psi(\vec{\Omega}')\,d\vec{\Omega}' + S^e(\vec{\Omega}). \qquad (2.15a)$$

Similarly, the subtraction of the same two equations yields

$$\vec{\Omega}\cdot\vec{\nabla}\ \psi(\vec{\Omega}) + \Sigma\chi(\vec{\Omega}) = \int_{\vec{\Omega}'} \Sigma_s^0(\vec{\Omega}'\cdot\vec{\Omega})\ \chi(\vec{\Omega}')\ d\vec{\Omega}' + S^0(\vec{\Omega}). \qquad (2.15b)$$

This form of the neutron transport equation is referred to as the canonical transport equation.[18]

The Even-Parity Form of the Transport Equation

Equation (2.15) can now be combined to form two second order equations. The second order equation is the even-parity flux, which is of interest in this work, can be obtained in the following manner.

Rewrite Equation (2.15b) as

$$H\chi(\vec{\Omega}) = -\vec{\Omega}\cdot\vec{\nabla}\psi(\vec{\Omega}) + S^0(\vec{\Omega}), \qquad (2.16)$$

where H is an operator defined as follows:

$$H\chi(\vec{\Omega}) = \Sigma\chi(\vec{\Omega}) - \int_{\vec{\Omega}'} \Sigma_s^0(\vec{\Omega}'\cdot\vec{\Omega})\ \chi(\vec{\Omega}')\ d\vec{\Omega}'. \qquad (2.17)$$

Therefore,

$$\chi(\vec{\Omega}) = H^{-1}[-\vec{\Omega}\cdot\vec{\nabla}\psi(\vec{\Omega}) + S^0(\vec{\Omega})]. \qquad (2.18)$$

To obtain the operator, H^{-1}, expand the scattering cross section, Σ_s, in Legendre Polynomials as follows,

$$\Sigma_s(\vec{\Omega}'\cdot\vec{\Omega}) = \sum_{\ell=0}^{\infty} \frac{2\ell+1}{4\pi}\ \Sigma_{s,\ell}\ P_\ell(\vec{\Omega}'\cdot\vec{\Omega}) \qquad (2.19)$$

where $\Sigma_{s,\ell}$ is the ℓ^{th} term in the series expansion,

$$P_\ell(\vec{\Omega}'\cdot\vec{\Omega}) = \frac{4\pi}{2\ell+1} \sum_{m=-\ell}^{\ell} Y_{\ell,m}(\vec{\Omega})\ Y^+_{\ell,m}(\vec{\Omega}')^*, \tag{2.20}$$

and $Y_{\ell,m}(\vec{\Omega})$ are surface harmonics which are defined elsewhere.[19]

Substitution of Equation (2.20) into Equation (2.19) yields

$$\Sigma_s(\vec{\Omega}'\cdot\vec{\Omega}) = \sum_{\ell=0}^{\infty} \Sigma_{s,\ell} \sum_{m=-\ell}^{\ell} Y_{\ell,m}(\vec{\Omega})\ Y^+_{\ell,m}(\vec{\Omega}'). \tag{2.21}$$

At this point, it should be noted that for even functions Equation (2.21) has nonzero coefficients for only even values of ℓ. It should also be remembered that

$$P_\ell(\vec{\Omega}'\cdot\vec{\Omega}) = P_\ell(\vec{\Omega}\cdot\vec{\Omega}'). \tag{2.22}$$

Noting these facts, the even and odd-parity scattering cross sections can be defined as

$$\Sigma_s^e(\vec{\Omega}'\cdot\vec{\Omega}) = \sum_{\ell \text{ even}} \Sigma_{s,\ell} \sum_{m=-\ell}^{\ell} Y_{\ell,m}(\vec{\Omega})\ Y^+_{\ell,m}(\vec{\Omega}'). \tag{2.23}$$

and

$$\Sigma_s^o(\vec{\Omega}'\cdot\vec{\Omega}) = \sum_{\ell \text{ odd}} \Sigma_{s,\ell} \sum_{m=-\ell}^{\ell} Y_{\ell,m}(\vec{\Omega})\ Y^+_{\ell,m}(\vec{\Omega}'). \tag{2.24}$$

Substitution of these results into Equation (2.17) gives

$$H\chi(\vec{\Omega}) = \Sigma\chi(\vec{\Omega}) - \sum_{\ell \text{ odd}} \Sigma_{s,\ell} \sum_{m=-\ell}^{\ell} Y_{\ell,m}(\vec{\Omega}) \int_{\vec{\Omega}'} Y^+_{\ell,m}(\vec{\Omega}')\ \chi(\vec{\Omega}')\ d\vec{\Omega}'. \tag{2.25}$$

Equation (2.25) is multiplied by $Y^+_{\ell',m'}(\vec{\Omega})$ and integrated over all $\vec{\Omega}$ space. Noting that

$$\int_{\vec{\Omega}'} Y_{\ell,m}(\vec{\Omega})\ Y^+_{\ell,m}(\vec{\Omega})\ d\vec{\Omega} = \delta_\ell^{\ell'}\ \delta_m^{m'} \tag{2.26}$$

---

*The superscript "+" denotes the complex conjugate of the function of interest.

where $\delta_{\ell}^{\ell'}$ and $\delta_{m}^{m'}$ are the Kronecker delta function. The resultant equation is

$$\int_{\vec{\Omega}'} G(\vec{\Omega})\ Y^{+}_{\ell',m'}(\vec{\Omega})\ d\vec{\Omega} = \Sigma \int_{\vec{\Omega}'} Y^{+}_{\ell',m'}(\vec{\Omega})\ \chi(\vec{\Omega})\ d\vec{\Omega} -$$

$$\sum_{\ell\ \text{odd}} \Sigma_{s,\ell} \sum_{m=-\ell}^{\ell} \int_{\vec{\Omega}} Y^{+}_{\ell,m}(\vec{\Omega}')\ \chi(\vec{\Omega}')\ d\vec{\Omega}', \tag{2.27}$$

where

$$G(\vec{\Omega}) = H\chi(\vec{\Omega}). \tag{2.28}$$

Since $\vec{\Omega}$ and $\vec{\Omega}'$ are only variables of integration

$$\int_{\vec{\Omega}} Y^{+}_{\ell,m}(\vec{\Omega})\ \chi(\vec{\Omega})\ d\vec{\Omega} = \int_{\vec{\Omega}'} Y^{+}_{\ell,m}(\vec{\Omega}')\ \chi(\vec{\Omega}')\ d\vec{\Omega}'. \tag{2.29}$$

Equation (2.27) can now be written as

$$\int_{\vec{\Omega}} G(\vec{\Omega})\ Y^{+}_{\ell,m}(\vec{\Omega})\ d\vec{\Omega} = \sum_{\ell\ \text{odd}} (\Sigma - \Sigma_{s,\ell}) \sum_{m=-\ell}^{\ell} \int_{\vec{\Omega}'} Y^{+}_{\ell,m}(\vec{\Omega}')\ \chi(\vec{\Omega}')\ d\vec{\Omega}', \tag{2.30}$$

or upon rearrangement as

$$\int_{\vec{\Omega}'} Y^{+}_{\ell,m}(\vec{\Omega}')\ \chi(\vec{\Omega}')\ d\vec{\Omega}' = \sum_{\ell\ \text{odd}} \frac{1}{\Sigma - \Sigma_{s,\ell}} \sum_{m=-\ell}^{\ell} \int_{\vec{\Omega}} G(\vec{\Omega})\ Y^{+}_{\ell,m}(\vec{\Omega})\ d\vec{\Omega}. \tag{2.31}$$

Now substitute Equation (2.31) into Equation (2.25) to obtain

$$H\chi(\vec{\Omega}) = G(\vec{\Omega}) = \Sigma\chi(\vec{\Omega}) -$$

$$\sum_{\ell\ \text{odd}} \frac{\Sigma_{s,\ell}}{\Sigma - \Sigma_{s,\ell}} \sum_{m=-\ell}^{\ell} Y_{\ell,m}(\vec{\Omega}) \int_{\vec{\Omega}'} Y^{+}_{\ell,m}(\vec{\Omega}')\ H\chi(\vec{\Omega}')\ d\vec{\Omega}'. \tag{2.32}$$

Now substitute Equation (2.16) into the integral in Equation (2.25) and rearrange to obtain

$$\chi(\vec{\Omega}) = \frac{-\vec{\Omega}\cdot\vec{\nabla}\ \psi(\vec{\Omega}) + S^{o}(\vec{\Omega})}{\Sigma} +$$

$$\frac{1}{\Sigma} \sum_{\ell\ \text{odd}} \frac{\Sigma_{s,\ell}}{\Sigma-\Sigma_{s,\ell}} \sum_{m=-\ell}^{\ell} Y_{\ell,m}(\vec{\Omega}) \int_{\vec{\Omega}'} Y^{+}_{\ell,m}(\vec{\Omega}') \left[-\vec{\Omega}'\cdot\vec{\nabla}\psi(\vec{\Omega}') + S^{o}(\vec{\Omega}')\right] d\vec{\Omega}'. \tag{2.33}$$

Using the expansions for the cross sections defined by Equations (2.23) and (2.24), Equation (2.15a) can now be rewritten as

$$-\vec{\Omega}\cdot\vec{\nabla}\ \chi(\vec{\Omega}) = \Sigma\psi(\vec{\Omega}) -$$

$$\sum_{\ell=0}^{\infty} \Sigma_{s,\ell} \sum_{m=-\ell}^{\ell} Y_{\ell,m}(\vec{\Omega}) \int_{\vec{\Omega}'} Y^{+}_{\ell,m}(\vec{\Omega}')\ \psi(\vec{\Omega}')\ d\vec{\Omega}' - S^{e}(\vec{\Omega}). \tag{2.34}$$

Equation (2.33) can now be substituted into Equation (2.34) to yield the following second order form of the even-parity transport equation,

$$\frac{\vec{\Omega}\cdot\vec{\nabla}[\vec{\Omega}\cdot\vec{\nabla}\ \psi(\vec{\Omega})]}{\Sigma} - \frac{\vec{\Omega}\cdot\vec{\nabla}\ S^{o}(\vec{\Omega})}{\Sigma} -$$

$$\frac{-\vec{\Omega}\cdot\vec{\nabla}}{\Sigma}\left\{ \sum_{\ell\ \text{odd}} \frac{\Sigma_{s,\ell}}{\Sigma-\Sigma_{s,\ell}} \sum_{m=-\ell}^{\ell} Y_{\ell,m}(\vec{\Omega}) \int_{\vec{\Omega}'} Y^{+}_{\ell,m}(\vec{\Omega}')[S^{o}(\vec{\Omega}') - \vec{\Omega}'\cdot\vec{\nabla}'\psi(\vec{\Omega}')]\ d\vec{\Omega}'\right\} -$$

$$\Sigma\psi(\vec{\Omega}) + \sum_{\ell\ \text{even}} \Sigma_{s,\ell} \sum_{m=-\ell}^{\ell} Y_{\ell,m}(\vec{\Omega}) \int_{\vec{\Omega}'} Y^{+}_{\ell,m}(\vec{\Omega}')\ \psi(\vec{\Omega}')\ d\vec{\Omega}' +$$

$$S^{e}(\vec{\Omega}) = 0. \tag{2.35}$$

The Even-Parity Functional

The advantages of using variational techniques to obtain the set of algebraic equations to be solved were discussed in Chapter I, page 4. It is of interest to construct a functional whose first variation with respect to the unknown function, ψ in this case, gives Equation (2.35) as its Euler Equation. To accomplish this, introduce the idea of the variational derivative,[20] δ, defined as

$$\delta F(\psi) = \lim_{\epsilon \to 0} \frac{\partial}{\partial \epsilon} F(\psi + \epsilon \delta \psi). \tag{2.36}$$

The equation for the first variation of the functional can be written as

$$\delta F(\psi) = \int_{\vec{r}} \int_{\vec{\Omega}} \delta\psi(\vec{\Omega}) \left\{ \frac{\vec{\Omega}\cdot\vec{\nabla}[\vec{\Omega}\cdot\vec{\nabla}\psi(\vec{\Omega})]}{\Sigma} - \frac{\vec{\Omega}\cdot\vec{\nabla}\, S^o(\vec{\Omega})}{\Sigma} - \right.$$

$$\frac{\vec{\Omega}\cdot\vec{\nabla}}{\Sigma} \left[\sum_{\ell \text{ odd}} \frac{\Sigma_{s,\ell}}{\Sigma - \Sigma_{s,\ell}} \sum_{m=-\ell}^{\ell} Y_{\ell,m}(\vec{\Omega}) \int_{\vec{\Omega}'} Y^+_{\ell,m}(\vec{\Omega}') \{S^o(\vec{\Omega}') - \vec{\Omega}'\cdot\vec{\nabla}\psi(\vec{\Omega}')\}\, d\vec{\Omega}' \right] -$$

$$\left. \Sigma\psi(\vec{\Omega}) + \sum_{\ell \text{ even}} \Sigma_{s,\ell} \sum_{m=-\ell}^{\ell} Y_{\ell,m}(\vec{\Omega}) \int_{\vec{\Omega}'} Y^+_{\ell,m}(\vec{\Omega}')\, \psi(\vec{\Omega}')\, d\vec{\Omega}' + S^e(\vec{\Omega}) \right\} d\vec{\Omega} d\vec{r} \tag{2.37}$$

where $\vec{r}$ denotes the entire solution domain.

Operating on Equation (2.37) with the following vector identities[21]

$$\vec{\Omega}\cdot\vec{\nabla} f = \vec{\nabla}\cdot\vec{\Omega} f \tag{2.38}$$

and

$$u\vec{\Omega}\cdot\vec{\nabla} f = \vec{\nabla}\cdot[u\vec{\Omega} f] - [\vec{\Omega}\cdot\vec{\nabla} u] f \tag{2.39}$$

yields the following functional,

$$F(\psi) = \frac{1}{2} \int_{\vec{r}} \int_{\vec{\Omega}} \{\frac{[\vec{\Omega}\cdot\vec{\nabla}\psi(\vec{\Omega})]^2}{\Sigma} + \Sigma\psi(\vec{\Omega})^2 -$$

$$\psi(\vec{\Omega}) \sum_{\ell \text{ even}} \Sigma_{s,\ell} \sum_{m=-\ell}^{\ell} Y_{\ell,m}(\vec{\Omega}) \int_{\vec{\Omega}'} Y^{+}_{\ell,m}(\vec{\Omega}')\ \psi(\vec{\Omega}')d\vec{\Omega}' +$$

$$\vec{\Omega}\cdot\vec{\nabla}\psi(\vec{\Omega}) \int_{\Omega'} g(\vec{\Omega}'\cdot\vec{\Omega})\ \vec{\Omega}'\cdot\vec{\nabla}\psi(\vec{\Omega}')\ d\vec{\Omega}' - \frac{2\vec{\Omega}\cdot\vec{\nabla}\psi(\vec{\Omega})\ S^{o}(\vec{\Omega})}{\Sigma} -$$

$$2\psi(\vec{\Omega})\ S^{e}(\vec{\Omega}) - 2\vec{\Omega}\cdot\vec{\nabla}\psi(\vec{\Omega}) \int_{\Omega'} g(\vec{\Omega}'\cdot\vec{\Omega})\ S^{o}(\vec{\Omega}')\ d\vec{\Omega}'\} \ d\vec{\Omega}d\vec{r} +$$

$$\int_{\vec{r}} \int_{\vec{\Omega}} \vec{\nabla}\cdot\delta\psi(\vec{\Omega})\vec{\Omega}[\frac{-\vec{\Omega}\cdot\vec{\nabla}\psi(\vec{\Omega})}{\Sigma} + \frac{S^{o}(\vec{\Omega})}{\Sigma} -$$

$$\int_{\vec{\Omega}'} g(\vec{\Omega}'\cdot\vec{\Omega})\ \vec{\Omega}'\cdot\vec{\nabla}\psi(\vec{\Omega}')\ d\vec{\Omega}' + \int_{\vec{\Omega}'} g(\vec{\Omega}'\cdot\vec{\Omega})\ S^{o}(\vec{\Omega}')\ d\vec{\Omega}'] \ d\vec{\Omega}d\vec{r} \qquad (2.40)$$

where

$$g(\vec{\Omega}'\cdot\vec{\Omega}) = \frac{1}{\Sigma} \sum_{\ell \text{ odd}} \frac{\Sigma_{s,\ell}}{\Sigma-\Sigma_{s,\ell}} \sum_{m=-\ell}^{\ell} Y_{\ell,m}(\vec{\Omega})\ Y^{+}_{\ell,m}(\vec{\Omega}'). \qquad (2.41)$$

The terms in brackets in the second integral over $\vec{\Omega}$ in Equation (2.40) is equivalent to Equation (2.33). Therefore, Equation (2.40) can be written as

$$F(\psi) = \frac{1}{2} \int_{\vec{r}} \int_{\vec{\Omega}} \{\frac{[\vec{\Omega}\cdot\vec{\nabla}\psi(\vec{\Omega})]^2}{\Sigma} + \Sigma\psi(\vec{\Omega})^2 -$$

$$\psi(\vec{\Omega}) \sum_{\ell \text{ even}} \Sigma_{s,\ell} \sum_{m=-\ell}^{\ell} Y_{\ell,m}(\vec{\Omega}) \int_{\vec{\Omega}'} Y^{+}_{\ell,m}(\vec{\Omega}')\ \psi(\vec{\Omega}')\ d\vec{\Omega}' +$$

$$\vec{\Omega}\cdot\vec{\nabla}\psi(\vec{\Omega}) \int_{\vec{\Omega}'} g(\vec{\Omega}'\cdot\vec{\Omega})\ \vec{\Omega}'\cdot\vec{\nabla}\psi(\vec{\Omega}')\ d\vec{\Omega}' - \frac{2\vec{\Omega}\cdot\vec{\nabla}\psi(\vec{\Omega})\ S^o(\vec{\Omega})}{\Sigma} -$$

$$2\psi(\vec{\Omega})\ S^e(\vec{\Omega}) - 2\vec{\Omega}\cdot\vec{\nabla}\psi(\vec{\Omega}) \int_{\vec{\Omega}} g(\vec{\Omega}'\cdot\vec{\Omega})\ S^o(\vec{\Omega}')\ d\vec{\Omega}' \}\ d\vec{\Omega}d\vec{r} +$$

$$\int_{\vec{r}} \int_{\vec{\Omega}} \vec{\nabla}\cdot[\delta\psi(\vec{\Omega})\vec{\Omega}\chi(\vec{\Omega})]\ d\vec{\Omega}d\vec{r}. \qquad (2.42)$$

Since $\psi(\vec{\Omega})$ and $\chi(\vec{\Omega})$ are both continuous functions in phase-space over the region $\vec{r}$ Green's Theorem can be applied to the last integral in Equation (2.42) as follows,

$$\int_{\vec{r}} \int_{\vec{\Omega}} \vec{\nabla}\cdot[\delta\psi(\vec{\Omega})\vec{\Omega}\chi(\vec{\Omega})]\ d\vec{\Omega}d\vec{r} = \int_{\vec{\Gamma}} \int_{\vec{\Omega}} \delta\psi(\vec{\Omega})\ \vec{\Omega}\cdot\vec{n}\ \chi(\vec{\Omega})\ d\vec{\Omega}d\vec{\Gamma}, \qquad (2.43)$$

where $\vec{\Gamma}$ represents all the external surfaces of the solution domain and $\vec{n}$ is a unit vector normal to $\vec{\Gamma}$.

At this point, it becomes necessary to examine the effects of some common boundary conditions on the form of the functional For the nonreturn boundary

$$\phi(\vec{\Omega}) = 0. \quad \text{For } \vec{\Omega}\cdot\vec{n} < 0, \qquad (2.44)$$

which, in terms of the even and odd-parity fluxes can be written as

$$\psi(\vec{\Omega}) + \chi(\vec{\Omega}) = 0. \quad \text{For } \vec{\Omega}\cdot\vec{n} < 0 \qquad (2.45a)$$

and

$$\psi(\vec{\Omega}) - \chi(\vec{\Omega}) = 0. \quad \text{For } \vec{\Omega}\cdot\vec{n} > 0. \qquad (2.45b)$$

Equation (2.43) can be rewritten as

$$\int_{\vec{\Gamma}} \int_{\vec{\Omega}} \delta\psi(\vec{\Omega})\ \vec{\Omega}\cdot\vec{n}\ \chi(\vec{\Omega})\ d\vec{\Omega}d\vec{\Gamma} =$$

$$\int_{\vec{\Gamma}} \int_{\vec{\Omega}\cdot\vec{n}<0} \delta\psi(\vec{\Omega})\ \vec{\Omega}\cdot\vec{n}\ \chi(\vec{\Omega})\ d\vec{\Omega}d\vec{\Gamma} + \int_{\vec{\Gamma}} \int_{\vec{\Omega}\cdot\vec{n}>0} \delta\psi(\vec{\Omega})\ \vec{\Omega}\cdot\vec{n}\ \chi(\vec{\Omega})\ d\vec{\Omega}d\vec{\Gamma}. \qquad (2.46)$$

Applying Equations (2.45) gives

$$\int_{\vec{\Gamma}} \int_{\vec{\Omega}\cdot\vec{n}<0} \delta\psi(\vec{\Omega})\ \vec{\Omega}\cdot\vec{n}[-\psi(\vec{\Omega})]\ d\vec{\Omega}d\vec{\Gamma} + \int_{\vec{\Gamma}} \int_{\vec{\Omega}\cdot\vec{n}>0} \delta\psi(\vec{\Omega})\ \vec{\Omega}\cdot\vec{n}[\psi(\vec{\Omega})]\ d\vec{\Omega}d\vec{\Gamma} =$$

$$\int_{\vec{\Gamma}} \int_{\vec{\Omega}} \delta\psi(\vec{\Omega})|\vec{\Omega}\cdot\vec{n}|\psi(\vec{\Omega})\ d\vec{\Omega}d\vec{\Gamma} = \frac{\delta}{2} \int_{\vec{\Gamma}} \int_{\vec{\Omega}} |\vec{\Omega}\cdot\vec{n}|\psi(\vec{\Omega})^2\ d\vec{\Omega}d\vec{\Gamma} \qquad (2.47)$$

as the appropriate term to be included in the functional for nonreturn boundaries.

The second type of boundary condition considered is the symmetric boundary condition.

For symmetric boundaries

$$\phi(\vec{\Omega}_r) = \phi(\vec{\Omega}), \qquad (2.48)$$

where $\vec{\Omega}_r$ is the reflected direction vector. This can be written as

$$\psi(\vec{\Omega}_r) = \psi(\vec{\Omega}) \qquad (2.49a)$$

and

$$\chi(\vec{\Omega}_r) = \chi(\vec{\Omega}) \qquad (2.49b)$$

in terms of the even and odd-parity fluxes.

Equation (2.46) can be written as

$$\int_{\vec{\Gamma}} \int_{\vec{\Omega}} \delta\psi(\vec{\Omega})\ \vec{\Omega}\cdot\vec{n}\ \chi(\vec{\Omega})\ d\vec{\Omega}d\vec{\Gamma} =$$

$$\int_{\vec{\Gamma}} \int_{\vec{\Omega}\cdot\vec{n}>0} \delta\psi(\vec{\Omega})\ \vec{\Omega}\cdot\vec{n}\ \chi(\vec{\Omega})\ d\vec{\Omega}d\vec{\Gamma} + \int_{\vec{\Gamma}} \int_{\vec{\Omega}\cdot\vec{n}<0} \delta\psi(\vec{\Omega})\ \vec{\Omega}\cdot\vec{n}\ \chi(\vec{\Omega})\ d\vec{\Omega}d\vec{\Gamma}. \qquad (2.50)$$

It is also known that

$$\vec{\Omega}\cdot\vec{n} = -\vec{\Omega}_r\cdot\vec{n} \qquad (2.51)$$

which is evident from Figure 1. Therefore,

$$\int_{\vec{\Gamma}} \int_{\vec{\Omega}_r \cdot \vec{n} < 0} \delta\psi(\vec{\Omega}_r)\, \vec{\Omega}_r \cdot \vec{n}\, \chi(\vec{\Omega}_r)\, d\vec{\Omega}_r d\vec{\Gamma} = -\int_{\vec{\Gamma}} \int_{\vec{\Omega}_r \cdot \vec{n} > 0} \delta\psi(\vec{\Omega})\, \vec{\Omega} \cdot \vec{n}\, \chi(\vec{\Omega})\, d\vec{\Omega} d\vec{\Gamma}. \tag{2.52}$$

Substitution of this result into Equation (2.50) and using Equations (2.49) yields

$$\int_{\vec{\Gamma}} \int_{\vec{\Omega}} \delta\psi(\vec{\Omega})\, \vec{\Omega} \cdot \vec{n} [\chi(\vec{\Omega}) - \chi(\vec{\Omega}_r)]\, d\vec{\Omega} d\vec{\Gamma} = 0. \tag{2.53}$$

The even-parity functional can now be written as

$$F(\psi) = \frac{1}{2} \int_{\vec{r}} \int_{\vec{\Omega}} \{ \frac{[\vec{\Omega} \cdot \vec{\nabla} \psi(\vec{\Omega})]^2}{\Sigma} + \Sigma \psi(\vec{\Omega})^2 -$$

$$\psi(\vec{\Omega}) \sum_{\ell \text{ even}} \Sigma_{s,\ell} \sum_{m=-\ell}^{\ell} Y_{\ell,m}(\vec{\Omega}) \int_{\vec{\Omega}'} Y^{+}_{\ell,m}(\vec{\Omega}')\, \psi(\vec{\Omega}')\, d\vec{\Omega}' +$$

$$\vec{\Omega} \cdot \vec{\nabla} \psi(\vec{\Omega}) \int_{\vec{\Omega}'} g(\vec{\Omega}' \cdot \vec{\Omega})\, \vec{\Omega}' \cdot \vec{\nabla}\, \psi(\vec{\Omega}') - \frac{2\vec{\Omega} \cdot \vec{\nabla} \psi(\vec{\Omega})\, S^{o}(\vec{\Omega})}{\Sigma} -$$

$$2\psi(\vec{\Omega})\, S^{e}(\vec{\Omega}) - 2\vec{\Omega} \cdot \vec{\nabla} \psi(\vec{\Omega}) \int_{\vec{\Omega}} g(\vec{\Omega}' \cdot \vec{\Omega})\, S^{o}(\vec{\Omega}')\, d\vec{\Omega}' \} \, d\vec{\Omega} d\vec{r} +$$

$$\frac{\gamma}{2} \int_{\vec{\Gamma}} \int_{\vec{\Omega}} |\vec{\Omega} \cdot \vec{n}|\, \psi(\vec{\Omega})^2\, d\vec{\Omega} d\vec{\Gamma}, \tag{2.54}$$

where

γ = 0 for symmetric boundaries

1 for nonreturn boundaries.

When applying the symmetric boundary condition to Equation (2.42) to obtain Equation (2.54), it is not necessary to use the $\psi(\vec{\Omega})$ constraint equation, Equation (2.49a). Therefore, it is necessary to consider the variation of the odd-parity function to obtain the

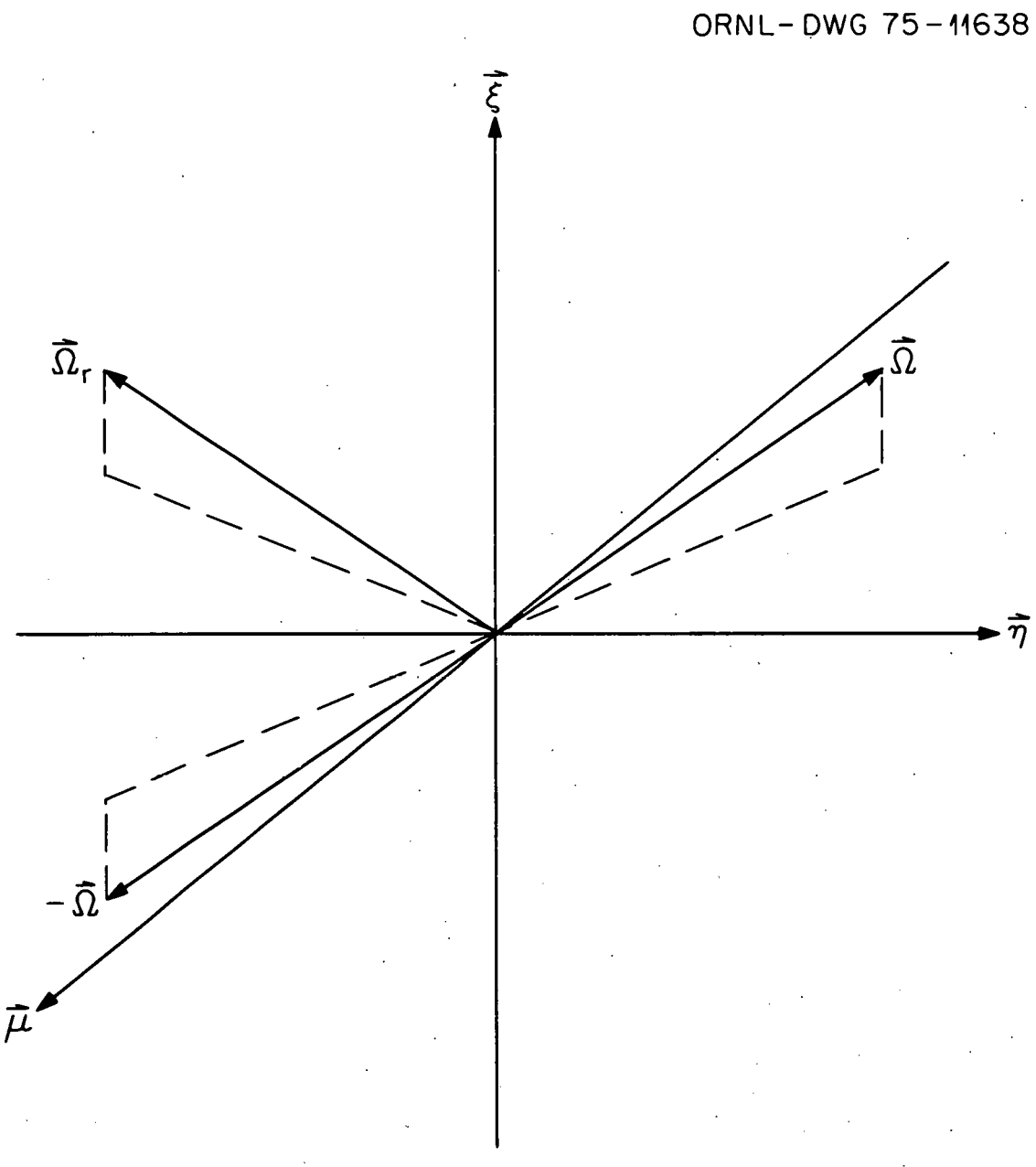

Figure 1. Reflected Angle $\vec{\Omega}_r$ in the ξ-η-μ Coordinate System.

essential boundary conditions, if any, that should be imposed on the even-parity functional.

The odd-parity functional is obtained through a procedure similar to that used to obtain the even-parity functional or by envoking an involutory transformation.[18,22] The odd-parity functional is

$$F(\chi) = -\frac{1}{2} \int_{\vec{r}} \int_{\vec{\Omega}} \{\frac{[\vec{\Omega}\cdot\vec{\nabla}\chi(\vec{\Omega})]^2}{\Sigma} + \Sigma\chi(\vec{\Omega})^2 -$$

$$\chi(\vec{\Omega}) \sum_{\ell \text{ odd}} \Sigma_{s,\ell} \sum_{m=-\ell}^{\ell} Y_{\ell,m}(\vec{\Omega}) \int_{\vec{\Omega}'} Y^{+}_{\ell,m}(\vec{\Omega}')\ \chi(\vec{\Omega}')\ d\vec{\Omega}' +$$

$$\vec{\Omega}\cdot\vec{\nabla}\ \chi(\vec{\Omega}) \int_{\vec{\Omega}'} g(\vec{\Omega}'\cdot\vec{\Omega})^*\ \vec{\Omega}'\cdot\vec{\nabla}\ \chi(\vec{\Omega}')\ d\vec{\Omega}' - \frac{2\vec{\Omega}\cdot\vec{\nabla}\chi(\vec{\Omega})\ S^3(\vec{\Omega})}{\Sigma} -$$

$$2\chi(\vec{\Omega})\ S^o(\vec{\Omega}) - 2\vec{\Omega}\cdot\vec{\nabla}\chi(\vec{\Omega}) \int_{\vec{\Omega}'} g(\vec{\Omega}'\cdot\vec{\Omega})^*\ S^e(\vec{\Omega}')\ d\vec{\Omega}'\} \ d\vec{\Omega}d\vec{r} -$$

$$\frac{\gamma}{2} \int_{\vec{\Gamma}} \int_{\vec{\Omega}} |\vec{\Omega}\cdot\vec{n}|\ \chi(\vec{\Omega})^2\ d\vec{\Omega}d\vec{\Gamma}, \qquad (2.55)$$

where $g(\vec{\Omega}'\cdot\vec{\Omega})^*$ is defined in the same manner as $g(\vec{\Omega}'\cdot\vec{\Omega})$ except the sum is over the odd values of ℓ instead of the even values of ℓ.

The first variation of Equation (2.55) with respect to $(\vec{\Omega})$ is

$$\delta F(\chi) = -\int_{\vec{r}} \int_{\vec{\Omega}} \delta\chi(\vec{\Omega}) \{\frac{\vec{\Omega}\cdot\vec{\nabla}[\vec{\Omega}\cdot\vec{\nabla}\chi(\vec{\Omega})]}{\Sigma} - \frac{\vec{\Omega}\cdot\vec{\nabla}\ S^e(\vec{\Omega})}{\Sigma} -$$

$$\Sigma\chi(\vec{\Omega}) + \sum_{\ell \text{ odd}} \Sigma_{s,\ell} \sum_{m=-\ell}^{\ell} Y_{\ell,m}(\vec{\Omega}) \int_{\vec{\Omega}'} Y^{+}_{\ell,m}(\vec{\Omega}')\ \chi(\vec{\Omega}')\ d\vec{\Omega}' -$$

$$\vec{\Omega}\cdot\vec{\nabla} \int_{\vec{\Omega}'} g(\vec{\Omega}'\cdot\vec{\Omega})^*\ [\vec{\Omega}'\cdot\vec{\nabla}\chi(\vec{\Omega}') - S^e(\vec{\Omega}')]\ d\vec{\Omega}' + S^o(\vec{\Omega})\} \ d\vec{\Omega}d\vec{r} -$$

$$\frac{\gamma}{2}\int_{\vec{\Gamma}}\int_{\vec{\Omega}}\delta\chi(\vec{\Omega})\,\vec{\Omega}\cdot\vec{n}\,\chi(\vec{\Omega})\,d\Omega d\vec{\Gamma}+\int_{\vec{r}}\int_{\vec{\Omega}}\vec{\nabla}\cdot\{\delta\chi(\vec{\Omega})\,\vec{\Omega}[\frac{-\vec{\Omega}\cdot\vec{\nabla}\chi(\vec{\Omega})}{\Sigma}+$$

$$\frac{S^{e}(\vec{\Omega})}{\Sigma}+\int_{\vec{\Omega}'}g(\vec{\Omega}'\cdot\vec{\Omega})^{*}\{-\vec{\Omega}'\cdot\vec{\nabla}\chi(\vec{\Omega}')+S^{e}(\vec{\Omega}')\}d\vec{\Omega}']\}d\vec{\Omega}d\vec{r}. \qquad (2.56)$$

The bracketed term in the third integral is $\psi(\vec{\Omega})$. Using Green's Theorem, Equation (2.56) can be written as

$$\delta F(\chi)=\int_{\vec{r}}\int_{\vec{\Omega}}\delta\chi(\vec{\Omega})\{\frac{\vec{\Omega}\cdot\vec{\nabla}[\vec{\Omega}\cdot\vec{\nabla}\chi(\vec{\Omega})]}{\Sigma}-\frac{\vec{\Omega}\cdot\vec{\nabla}\,S^{e}(\vec{\Omega})}{\Sigma}-$$

$$\Sigma\chi(\vec{\Omega})+\sum_{\ell\ \text{odd}}\Sigma_{s,\ell}\sum_{m=-\ell}^{\ell}Y_{\ell,m}(\vec{\Omega})\int_{\vec{\Omega}'}Y^{+}_{\ell,m}(\vec{\Omega}')\,\chi(\vec{\Omega}')\,d\vec{\Omega}'-$$

$$\vec{\Omega}\cdot\vec{\nabla}\int_{\vec{\Omega}'}g(\vec{\Omega}'\cdot\vec{\Omega})^{*}\,[S^{e}(\vec{\Omega}')-\vec{\Omega}'\cdot\vec{\nabla}\chi(\vec{\Omega}')]\,d\vec{\Omega}'+S^{o}(\vec{\Omega})\}\,d\vec{\Omega}d\vec{r}+$$

$$\frac{\gamma}{2}\int_{\vec{\Gamma}}\int_{\vec{\Omega}}\delta\chi(\vec{\Omega})|\vec{\Omega}\cdot\vec{n}|\,\chi(\vec{\Omega})\,d\vec{\Omega}d\vec{\Gamma}-\int_{\vec{\Gamma}}\int_{\vec{\Omega}}\delta\chi(\vec{\Omega})\,\vec{\Omega}\cdot\vec{n}\,\psi(\vec{\Omega})\,d\vec{\Omega}d\vec{\Gamma}. \qquad (2.57)$$

Consider the nonreturn boundary condition once again. Using the same procedure used to obtain Equation (2.54) it can be shown that the second surface integral is equal to the first. Therefore, their difference is equal to zero. Thus, the nonreturn boundary condition imposes no additional constraints on the even-parity functional.

For the symmetric boundary condition, substitute Equation (2.49a) into the second surface integral. As in the even-parity functional, the result is zero. It can therefore be concluded that both the nonreturn and the symmetric boundary conditions are natural conditions arising from the functional. That is, the

surface integral is included in the functional for nonreturn boundaries and deleted for symmetric boundaries.

The adjoint problem is often of interest in reactor physics studies. A discussion of the formulation of the adjoint problem is presented in Appendix A.

The Reduced Functional

The even and odd-parity fluxes are now expanded in surface harmonics.

$$\psi(X,Y,\vec{\Omega}) = \sum_{\ell \text{ even}} \sum_{m=-\ell}^{\ell} \psi_{\ell,m}(X,Y)\, Y_{\ell,m}(\vec{\Omega}) \tag{2.58}$$

$$\chi(X,Y,\vec{\Omega}) = \sum_{\ell \text{ odd}} \sum_{m=-\ell}^{\ell} \chi_{\ell,m}(X,Y)\, Y_{\ell,m}(\vec{\Omega}). \tag{2.59}$$

The scope of the remaining derivation is limited to the consideration of linearly anisotropic scattering and linearly anisotropic fluxes. The expansions for the fluxes and sources now degenerates to the following set of polynomials,

$$\psi(X,Y,\vec{\Omega}) = \psi_{0,0}(X,Y)\, Y_{0,0}(\vec{\Omega}), \tag{2.60a}$$

$$\chi(X,Y,\vec{\Omega}) = \chi_{1,-1}(X,Y)\, Y_{1,-1}(\vec{\Omega}) + \chi_{1,0}(X,Y)\, Y_{1,0}(\vec{\Omega}) + \chi_{1,1}(X,Y)\, Y_{1,1}(\vec{\Omega}), \tag{2.60b}$$

$$S^{e}(X,Y,\vec{\Omega}) = S_{0,0}(X,Y)\, Y_{0,0}(\vec{\Omega}), \tag{2.60c}$$

and

$$S^{o}(X,Y,\vec{\Omega}) = S_{1,-1}(X,Y)\, Y_{1,-1}(\vec{\Omega}) + S_{1,0}(X,Y)\, Y_{1,0}(\vec{\Omega}) + S_{1,1}(X,Y)\, Y_{1,1}(\vec{\Omega}). \tag{2.60d}$$

The substitution of Equations (2.60) into Equation (2.54) yields

$$F(\psi) = \frac{1}{2}\int_{\vec{r}}\int_{\vec{\Omega}} \frac{[\vec{\Omega}\cdot\vec{\nabla}\ \psi_{0,0}\ Y_{0,0}(\vec{\Omega})]^2}{\Sigma} + \Sigma[\psi_{0,0}\ Y_{0,0}(\vec{\Omega})]^2 -$$

$$\psi_{0,0}\ Y_{0,0}(\vec{\Omega})\ \Sigma_{s,0}\ Y_{0,0}(\vec{\Omega}) \int_{\vec{\Omega}'} Y^{+}_{0,0}(\vec{\Omega}')\ \psi_{0,0}\ d\vec{\Omega}' +$$

$$\vec{\Omega}\cdot\vec{\nabla}\ \psi_{0,0}\ Y_{0,0}(\vec{\Omega}) \int_{\vec{\Omega}'} g(\vec{\Omega}'\cdot\vec{\Omega})\ \vec{\Omega}'\cdot\vec{\nabla}\ \psi_{0,0}\ Y_{0,0}(\vec{\Omega}')\ d\vec{\Omega}' -$$

$$\frac{2\vec{\Omega}\cdot\vec{\nabla}\ \psi_{0,0}Y_{0,0}(\vec{\Omega})}{\Sigma}[S_{1,-1}Y_{1,-1}(\vec{\Omega}) + S_{1,0}Y_{1,0}(\vec{\Omega}) + S_{1,1}Y_{1,1}(\vec{\Omega})] -$$

$$2\ \psi_{0,0}\ Y_{0,0}(\vec{\Omega})\ S_{0,0}\ Y_{0,0}(\vec{\Omega}) -$$

$$2\vec{\Omega}\cdot\vec{\nabla}\ \psi_{0,0}\ Y_{0,0}(\vec{\Omega}) \int_{\vec{\Omega}'} g(\vec{\Omega}'\cdot\vec{\Omega})\ [S_{1,-1}Y_{1,-1}(\vec{\Omega}') + S_{1,0}Y_{1,0}(\vec{\Omega}') +$$

$$S_{1,1}Y_{1,1}(\vec{\Omega}')]\ d\vec{\Omega}'\}\ d\vec{\Omega}d\vec{r} +$$

$$\frac{\gamma}{2}\int_{\vec{\Gamma}}\int_{\vec{\Omega}} |\vec{\Omega}\cdot\vec{n}|\ \psi_{0,0}{}^2\ Y_{0,0}(\vec{\Omega})^2\ d\vec{\Omega}d\vec{\Gamma}, \qquad (2.61)$$

where

$$Y_{0,0} = \frac{1}{2\sqrt{\pi}}\ , \qquad (2.62a)$$

$$Y_{1,-1} = \sqrt{\frac{3}{8\pi}}\ \text{SIN}\ \theta\ e^{-i\phi}\ , \qquad (2.62b)$$

$$Y_{1,0} = \sqrt{\frac{3}{4\pi}}\ \text{COS}\ \theta, \qquad (2.62c)$$

$$Y_{1,1} = -\sqrt{\frac{3}{8\pi}}\ \text{SIN}\ \theta\ e^{i\phi}, \qquad (2.62d)$$

and

$$g(\vec{\Omega}'\cdot\vec{\Omega}) = \frac{\Sigma_{s,1}}{\Sigma(\Sigma-\Sigma_{s,1})} \sum_{m=-1}^{1} Y_{1,m}(\vec{\Omega})\, Y^{+}_{1,m}(\vec{\Omega}'). \tag{2.63}$$

The angles θ and ϕ are defined in Figure 2.

Equations (2.62) and Equation (2.63) are substituted into Equation (2.61) and the indicated integrations over $\vec{\Omega}$ and $\vec{\Omega}'$ are performed. The resultant functional is

$$F(\psi) = \frac{1}{2}\int_{\vec{r}} \{\frac{[\vec{\nabla}\,\psi_{0,0}]^2}{3\Sigma} + \Sigma\,\psi_{0,0}^{\,2} - \Sigma_{s,0}\psi_{0,0}^{\,2} + \frac{[\vec{\nabla}\,\psi_{0,0}]^2\,\Sigma_{s,1}}{3\Sigma(\Sigma-\Sigma_{s,1})}$$

$$\frac{2}{\Sigma}[\frac{1}{\sqrt{6}}\frac{\partial\psi_{0,0}}{\partial Y}S_{1,-1} + \frac{1}{\sqrt{3}}\frac{\partial\psi_{0,0}}{\partial X}S_{1,0} - \frac{1}{\sqrt{6}}\frac{\partial\psi_{0,0}}{\partial Y}S_{1,1}] -$$

$$2\,\psi_{0,0}S_{0,0} - \frac{2\,\Sigma_{s,1}}{\Sigma(\Sigma-\Sigma_{s,1})}[\frac{1}{\sqrt{6}}\frac{\partial\psi_{0,0}}{\partial Y}S_{1,-1} + \frac{1}{\sqrt{3}}\frac{\partial\psi_{0,0}}{\partial X}S_{1,0} -$$

$$\frac{1}{\sqrt{6}}\frac{\partial\psi_{0,0}}{\partial Y}S_{1,1}]\}\,d\vec{r} + \frac{\gamma}{4}\int_{\vec{\Gamma}} \psi_{0,0}^{\,2}\,d\vec{\Gamma}. \tag{2.64}$$

Rearrangement yields the following form of the reduced functional

$$F(\psi) = \frac{1}{2}\int_{\vec{r}} \{\frac{[\vec{\nabla}\psi_{0,0}]^2}{3(\Sigma-\Sigma_{s,1})} + (\Sigma-\Sigma_{s,0})\,\psi_{0,0}^{\,2} - 2\,\psi_{0,0}S_{0,0} -$$

$$\frac{2}{(\Sigma-\Sigma_{s,1})}[\frac{1}{\sqrt{6}}\frac{\partial\psi_{0,0}}{\partial Y}S_{1,-1} + \frac{1}{\sqrt{3}}\frac{\partial\psi_{0,0}}{\partial X}S_{1,0} - \frac{1}{\sqrt{6}}\frac{\partial\psi_{0,0}}{\partial Y}S_{1,1}]\}\,d\vec{r}$$

$$+ \frac{\gamma}{4}\int_{\vec{\Gamma}} \psi_{0,0}^{\,2}\,d\vec{\Gamma}. \tag{2.65}$$

Equation (2.65) can now be minimized and the even-parity flux calculated.

ORNL- DWG 75-11639

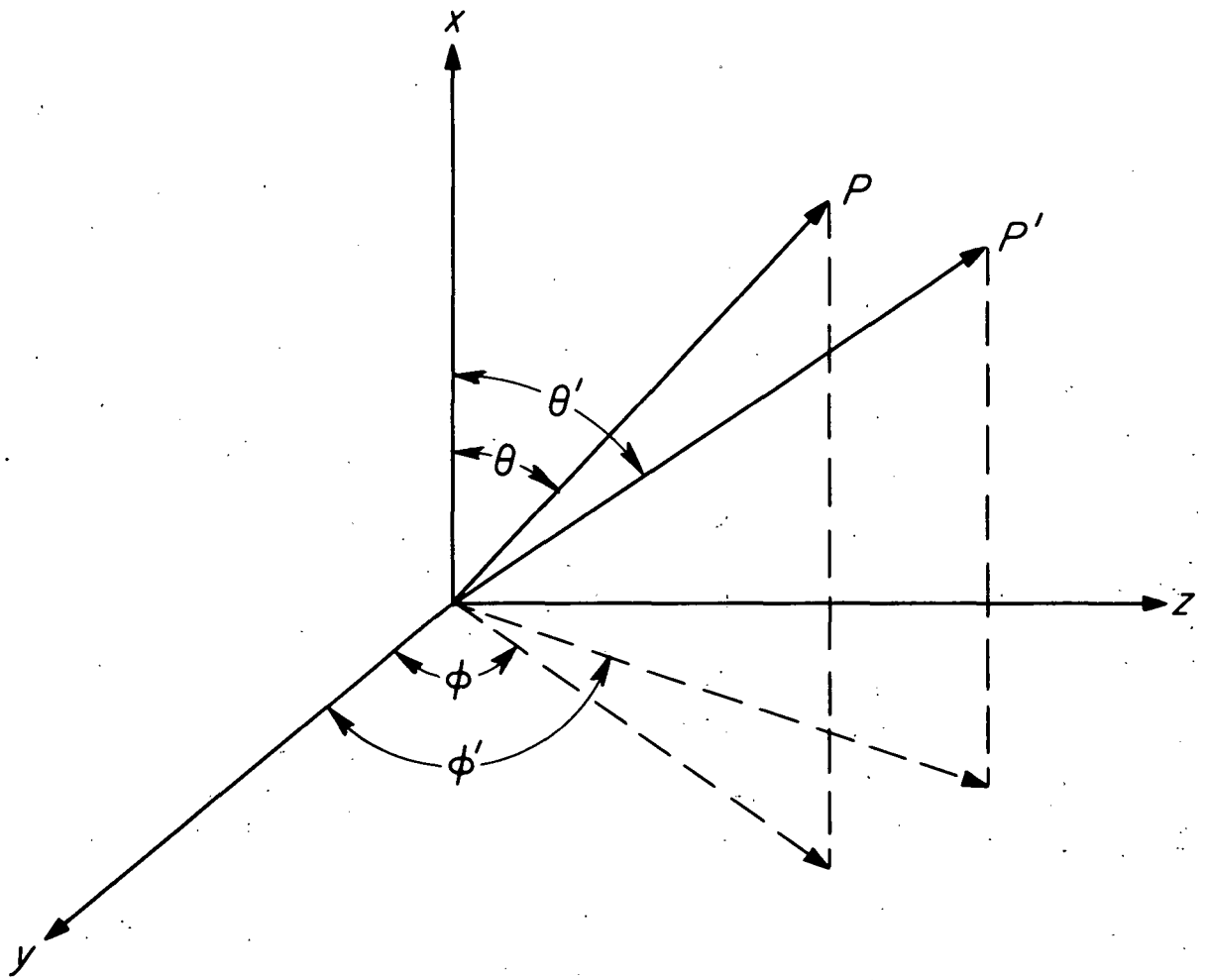

Figure 2. The Coordinate System in Rectangular Geometry.

The odd-parity flux can be obtained from Equation (2.33) once its reduced form is derived. For a P_1 expansion, Equation (2.33) takes the following form;

$$\chi(\vec{\Omega}) = \frac{S^o(\vec{\Omega})}{\Sigma} - \frac{\vec{\Omega}\cdot\vec{\nabla}\ \psi(\vec{\Omega})}{\Sigma} +$$

$$\frac{\Sigma_{s,1}}{\Sigma(\Sigma-\Sigma_{s,1})} \sum_{m=-1}^{1} Y_{1,m}(\vec{\Omega}) \int_{\vec{\Omega}'} Y^{+}_{1,m}(\vec{\Omega}') \left[S^o(\vec{\Omega}') - \vec{\Omega}'\cdot\vec{\nabla}\ \psi(\vec{\Omega}')\right] d\vec{\Omega}'. \tag{2.66}$$

Once again the fluxes and sources are expanded in surface harmonics as per Equations (2.60). These expansions are then substituted into Equation (2.66). The result is then multiplied through by $Y^{+}_{\ell',m'}(\vec{\Omega})$ and then integrated over all $\vec{\Omega}$. Using the orthogonal properties of the surface harmonics results in the following set of equations;

$$\chi_{1,-1} = \frac{1}{\Sigma-\Sigma_{s,1}}\left[-\frac{1}{\sqrt{6}}\frac{\partial\psi_{0,0}}{\partial Y} + S_{1,-1}\right], \tag{2.67a}$$

$$\chi_{1,0} = \frac{1}{\Sigma-\Sigma_{s,1}}\left[-\frac{1}{\sqrt{3}}\frac{\partial\psi_{0,0}}{\partial X} + S_{1,0}\right], \tag{2.67b}$$

and

$$\chi_{1,1} = \frac{1}{\Sigma-\Sigma_{s,1}}\left[\frac{1}{\sqrt{6}}\frac{\partial\psi_{0,0}}{\partial Y} + S_{1,1}\right]. \tag{2.67c}$$

Now that all the components of the real flux are known, it can be reconstructed in the following form;

$$\phi(\vec{\Omega}) = \frac{\psi_{0,0}}{2\sqrt{\pi}} + \chi_{1,0}\sqrt{\frac{3}{4\pi}}\,\mathrm{COS}\,\theta + \chi_{1,-1}\sqrt{\frac{3}{8\pi}}\,\mathrm{SIN}\,\theta\, e^{-i\phi} - \chi_{1,1}\sqrt{\frac{3}{8\pi}}\,\mathrm{SIN}\,\theta\, e^{i\phi}. \tag{2.68}$$

This can be rewritten as

$$\phi(\vec{\Omega}) = \frac{\psi_{0,0}}{2\sqrt{\pi}} + \chi_{1,0}\sqrt{\frac{3}{4\pi}}\,\mathrm{COS}\,\theta + \sqrt{\frac{3}{8\pi}}\,\mathrm{SIN}\,\theta\,\mathrm{COS}\,\phi[\chi_{1,-1} - \chi_{1,1}] - i\sqrt{\frac{3}{8\pi}}\,\mathrm{SIN}\,\theta\,\mathrm{SIN}\,\phi[\chi_{1,-1} + \chi_{1,1}]. \tag{2.69}$$

Since the flux is a real valued function

$$\chi_{1,1} = -\chi_{1,-1}. \tag{2.70}$$

Equation (2.69) can now be written as

$$\phi(\vec{\Omega}) = \frac{\psi_{0,0}}{2\sqrt{\pi}} + \chi_{1,0}\sqrt{\frac{3}{4\pi}}\,\mathrm{COS}\,\theta + \chi_{1,-1}\sqrt{\frac{3}{2\pi}}\,\mathrm{SIN}\,\theta\,\mathrm{COS}\,\phi. \tag{2.71}$$

The scalar flux is

$$\phi(X,Y) = \int_{\vec{\Omega}} \phi(\vec{\Omega})\, d\vec{\Omega} = 2\sqrt{\pi}\,\psi_{0,0}. \tag{2.72}$$

The substitution of Equation (2.70) into Equation (2.65) yields the final form of the reduced functional.

$$F(\psi) = \frac{1}{2} \int_{\vec{r}} \{ \frac{[\vec{\nabla}\psi_{0,0}]^2}{3(\Sigma-\Sigma_{s,1})} + (\Sigma-\Sigma_{s,0}) \psi_{0,0}^2 - 2 \psi_{0,0} S_{0,0} -$$

$$\frac{2}{(\Sigma-\Sigma_{s,1})} [\frac{2}{\sqrt{6}} \frac{\partial\psi_{0,0}}{\partial Y} S_{1,-1} + \frac{1}{\sqrt{3}} \frac{\partial\psi_{0,0}}{\partial X} S_{1,0}] \} \, d\vec{r} +$$

$$\frac{\gamma}{4} \int_{\vec{\Gamma}} \psi_{0,0}^2 \, d\vec{\Gamma}. \tag{2.73}$$

The multigroup even and odd-parity sources are now considered. Their derivation follows the same strategy used in the derivation of the canonical transport equations. For brevity, only the results are presented here.

$$S_g^e(\vec{\Omega}) = \frac{f_g}{4\pi} \sum_{g'=1}^{G} \nu\Sigma_{fg'} \int_{\vec{\Omega}'} \psi_{g'}(\vec{\Omega}') \, d\vec{\Omega}' +$$

$$\sum_{g'=1}^{g-1} \int_{\vec{\Omega}'} \Sigma_s^{e\ g'\to g}(\vec{\Omega}'\cdot\vec{\Omega}) \, \psi_{g'}(\vec{\Omega}') \, d\vec{\Omega}' + Q_g^e(\vec{\Omega}) \tag{2.74}$$

and

$$S_g^o(\vec{\Omega}) = \sum_{g'=1}^{g-1} \int_{\vec{\Omega}'} \Sigma_s^{o\ g'\to g}(\vec{\Omega}'\cdot\vec{\Omega}) \, \chi_{g'}(\vec{\Omega}') d\vec{\Omega}' + Q_g^o(\vec{\Omega}). \tag{2.75a}$$

where

$$Q_g^e = \frac{1}{2} [Q_g(\vec{\Omega}) + Q_g(-\vec{\Omega})] \tag{2.75b}$$

and

$$Q_g^o = \frac{1}{2} [Q_g(\vec{\Omega}) - Q_g(-\vec{\Omega})] \tag{2.75c}$$

Equations (2.60) are substituted into Equations (2.74) and (2.75a). Then the indicated integrations are performed resulting in the following set of equations;

$$S^g_{0,0} = f_g \sum_{g'=1}^{G} \nu\Sigma_{fg'} \psi^{g'}_{0,0} + \sum_{g'=1}^{g-1} \Sigma^{g'\to g}_{s,0} \psi^{g'}_{0,0} + Q^g_{0,0} , \tag{2.76}$$

$$S^g_{1,-1} = \sum_{g'=1}^{g-1} \Sigma^{g'\to g}_{s,1} \chi^{g'}_{1,-1} , \tag{2.77a}$$

$$S^g_{1,0} = \sum_{g'=1}^{g-1} \Sigma^{g'\to g}_{s,1} \chi^{g'}_{1,0} \tag{2.77b}$$

and by envoking Equation (2.70)

$$S^g_{1,1} = -S^g_{1,-1} . \tag{2.77c}$$

The odd-parity fixed source is set to zero for simplicity.

This completes the so-called "weak" formulation of the transport problem. It is termed weak because the family of functions that satisfy the functional must be continuous functions in the spatial domain and the first derivative must be square integrable, while the family of functions that satisfy the diffusion equation must be continuous and all the derivatives through the second must exist. This is a more stringent restriction on the even-parity flux than that imposed by the functional. However, this has been shown to have a minimal influence on the accuracy of the solution.[8]

II. The Finite Element Model

The solution domain is now divided into a number of smaller subdomains. Equation (2.65) is now approximated by a sum of integrals. The functional is now written as

$$F(\psi) = \frac{1}{2} \sum_{n=1}^{NE} \Big[\int_{\vec{r}_n} \Big\{ \frac{(\vec{\nabla}\psi_{0,0})^2}{3(\Sigma-\Sigma_{s,1})} + (\Sigma-\Sigma_{s,0})\ \psi_{0,0}^{\ 2} - 2\ \psi_{0,0} S_{0,0} - \frac{2}{(\Sigma-\Sigma_{s,1})} \Big[\frac{2}{\sqrt{6}} \frac{\partial \psi_{0,0}}{\partial Y} S_{1,-1} + \frac{1}{\sqrt{3}} \frac{\partial \psi_{0,0}}{\partial X} S_{1,0} \Big] \Big\}\, d\vec{r}_n + \frac{\gamma_n}{4} \int_{\vec{\Gamma}_n} \psi_{0,0}^{\ 2}\, d\vec{\Gamma}_n \Big], \tag{2.78}$$

where $\vec{r}_n$ and $\vec{\Gamma}_n$ are the areas and external surfaces, respectively, of each of the NE elements.

The subdomains are taken to be triangular in shape. A quadratic polynomial is used to describe the spatial variation of the even-parity flux over each triangular element. The reason for this choice of polynomial is discussed in Chapter I, page 6.

Therefore,

$$\psi_n(X,Y) = a_{1,n} + a_{2,n} X + a_{3,n} Y + a_{4,n} X^2 + a_{5,n} XY + a_{6,n} Y^2 \tag{2.79a}$$

or

$$\psi_n(X,Y) = [1 \quad X \quad Y \quad X^2 \quad XY \quad Y^2] \underline{a}^*_n \tag{2.79b}$$

or

$$\psi_n(X,Y) = \underline{f}^T \underline{a}_n \ . \tag{2.79c}$$

The double zero subscript has been deleted for simplicity.

For quadratic interpolating functions, it is necessary to describe the function in terms of six nodal points on the edges of each element. Three of these points, "nodes," are located at the vertices of the triangle and the remaining three are located at the mid-point of each side as illustrated in Figure 3. The variation of the flux is now expressed in terms of these nodal values as follows,

$$\begin{bmatrix} \psi_1 \\ \psi_2 \\ \psi_3 \\ \psi_4 \\ \psi_5 \\ \psi_6 \end{bmatrix} = \begin{bmatrix} 1 & X_1 & Y_1 & X_1^2 & X_1Y_1 & Y_1^2 \\ 1 & X_2 & Y_2 & X_2^2 & X_2Y_2 & Y_2^2 \\ 1 & X_3 & Y_3 & X_3^2 & X_3Y_3 & Y_3^2 \\ 1 & X_4 & Y_4 & X_4^2 & X_4Y_4 & Y_4^2 \\ 1 & X_5 & Y_5 & X_5^2 & X_5Y_5 & Y_5^2 \\ 1 & X_6 & Y_6 & X_6^2 & X_6Y_6 & Y_6^2 \end{bmatrix} \begin{bmatrix} a_1 \\ a_2 \\ a_3 \\ a_4 \\ a_5 \\ a_6 \end{bmatrix} \tag{2.80}$$

---

*Single underlined term denotes a vector and a doubly underlined term denotes a matrix.

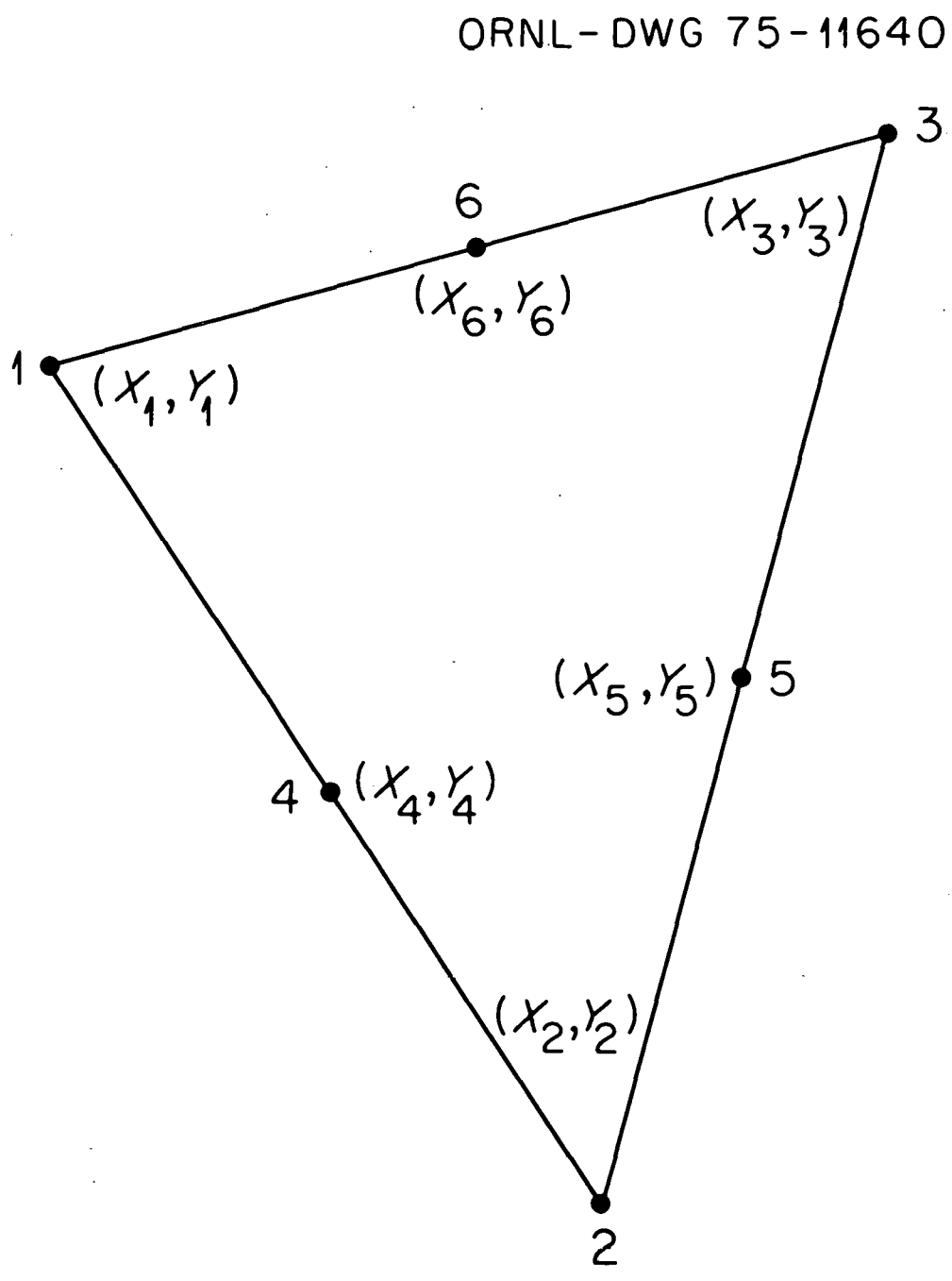

Figure 3. A Typical Triangular Element Illustrating the Nodal Numbering Scheme.

or symbolically

$$\bar{\underline{\psi}}_n = \underline{\underline{M}}\, \underline{a}_n. \tag{2.81}$$

Therefore,

$$\underline{a}_n = \underline{\underline{M}}^{-1}\, \bar{\underline{\psi}}_n. \tag{2.82}$$

Equation (2.82) is now substituted into Equation (2.79c). The results are

$$\psi_n(X,Y) = \underline{f}^T\, \underline{\underline{M}}^{-1}\, \bar{\underline{\psi}}_n. \tag{2.83}$$

This is now reduced to

$$\psi_n(X,Y) = \underline{N}^T\, \bar{\underline{\psi}}_n, \tag{2.84}$$

where $\bar{\underline{\psi}}_n$ is the element flux vector, the j^{th} element of which is the even-parity flux evaluated at the j^{th} node of the triangle and

$$\underline{N}^T = [N_1 \quad N_2 \quad N_3 \quad N_4 \quad N_5 \quad N_6]. \tag{2.85}$$

The elements of the N vector are defined as follows;

$$N_1 = (2\, L_1 - 1)\, L_1, \text{ etc.} \tag{2.86a}$$

for elements 1 through 3 and

$$N_4 = 4\, L_1\, L_2, \text{ etc.} \tag{2.86b}$$

for elements 4 through 6, where

$$L_i = (a_i + b_i\, X + c_i\, Y)/2\Delta, \tag{2.87}$$

$i = 1, 2, 3,$

$$a_1 = X_2 Y_3 - X_3 Y_2, \tag{2.88a}$$

$$b_1 = Y_2 - Y_3, \tag{2.88b}$$

and

$$c_1 = X_3 - X_2 \tag{2.88c}$$

and the remaining coefficients are permutations of these equations, i.e., 1 goes to 2, 2 to 3, and 3 to 1, and Δ is the area of the triangle.

Introduce a global flux vector, $\hat{\underline{\psi}}$, whose j^{th} component is the even-parity flux evaluated at the j^{th} node in the entire system. A Boolean matrix is used to relate the components in the element flux vector $\bar{\underline{\psi}}_n$ to their corresponding components in the global flux vector $\hat{\underline{\psi}}$. This Boolean matrix is defined as follows

$$J^n_{\ell,k} = \sum_{\ell'=1}^{6} \delta_{\ell}^{\ell'} \delta_{k}^{B^n_{\ell'}} \tag{2.89}$$

for $\ell = 1, 2, \ldots, 6$; $k = 1, 2, \ldots,$ NDF, and where $B^n_{\ell'}$ is a vector containing the global node number associated with node ℓ of element n, and NDF is the total number of nodes in the system. Therefore

$$\bar{\underline{\psi}}_n = \underline{\underline{J}}^n \hat{\underline{\psi}} \tag{2.90}$$

and

$$\psi_n(X,Y) = \underline{N}^T \underline{\underline{J}}^n \hat{\underline{\psi}}. \tag{2.91}$$

Similar arguments are advanced for the spatial variation of the sources and the results are

$$\bar{\underline{S}}^n_{0,0} = \underline{\underline{J}}^n \hat{\underline{S}}_{0,0}, \tag{2.92a}$$

$$\bar{\underline{S}}^n_{1,-1} = \underline{\underline{J}}^n \hat{\underline{S}}_{1,-1}, \tag{2.92b}$$

and

$$\bar{\underline{S}}^n_{1,0} = \underline{\underline{J}}^n \hat{\underline{S}}_{1,0}. \tag{2.92c}$$

Equation (2.91) and Equations (2.92) are now substituted into Equation (2.78). The result is

$$F(\psi) = \frac{1}{2}\hat{\underline{\psi}}^T \sum_{n=1}^{NE} [\underline{\underline{J}}^{n^T} \{\int_{\vec{r}_n} d\vec{r}_n [\frac{\vec{\nabla}\underline{N}(\vec{\nabla}\underline{N})^T}{3(\Sigma-\Sigma_{s,1})} + (\Sigma-\Sigma_{s,0})\,\underline{N}\,\underline{N}^T] +$$

$$\frac{\gamma_n}{4}\int_{\vec{\Gamma}_n} d\vec{\Gamma}_n \,\underline{N}\,\underline{N}^T\}\,\underline{\underline{J}}^n\,\hat{\underline{\psi}} - \int_{\vec{r}_n} d\vec{r}_n \{\frac{2}{(\Sigma-\Sigma_{s,1})}[\frac{2}{\sqrt{6}}\frac{\partial \underline{\underline{N}}}{\partial Y}\underline{N}^T\,\underline{\underline{J}}^n\,\hat{\underline{S}}_{1,-1} +$$

$$\frac{1}{\sqrt{3}}\frac{\partial \underline{\underline{N}}}{\partial X}\underline{N}^T\,\underline{\underline{J}}^n\,\hat{\underline{S}}_{1,0}] - 2\,\underline{N}\,\underline{N}^T\,\underline{\underline{J}}^n\,\hat{\underline{S}}_{0,0}\}]. \qquad (2.93)$$

The first variation of Equation (2.93) with respect to $\hat{\underline{\psi}}$ is taken and set equal to zero to obtain the stationary conditions of the functional. The resulting set of algebraic equations can be written symbolically as

$$\sum_{n=1}^{NE} [\underline{\underline{J}}^{n^T}\,\underline{\underline{A}}^n\,\underline{\underline{J}}^n\,\hat{\underline{\psi}}] = \sum_{n=1}^{NE} [\underline{\underline{J}}^{n^T}\,\underline{C}^n], \qquad (2.94)$$

where

$$\underline{\underline{A}}^n = \int_{\vec{r}_n} d\vec{r}_n [\frac{\vec{\nabla}\underline{N}(\vec{\nabla}\underline{N})^T}{3(\Sigma-\Sigma_{s,1})} + (\Sigma-\Sigma_{s,o})\,\underline{N}\,\underline{N}^T] + \frac{\gamma_n}{2}\int_{\vec{\Gamma}_n} d\vec{\Gamma}_n \,\underline{N}\,\underline{N}^T, \qquad (2.95)$$

and

$$\underline{C}^n = \int_{\vec{r}_n} d\vec{r}_n \{\underline{N}\,\underline{N}^T\,\underline{\underline{J}}^n\,\hat{\underline{S}}_{0,0} + \frac{1}{\Sigma-\Sigma_{s,1}}[\frac{2}{\sqrt{6}}\frac{\partial \underline{\underline{N}}}{\partial Y}\underline{N}^T\,\underline{\underline{J}}^n\,\hat{\underline{S}}_{1,-1} +$$

$$\frac{1}{\sqrt{3}}\frac{\partial \underline{\underline{N}}}{\partial X}\underline{N}^T\,\underline{\underline{J}}^n\,\hat{\underline{S}}_{1,0}]\}. \qquad (2.96)$$

The odd-parity element flux vectors are obtained by the substitution of Equation (2.91) and Equations (2.92) into Equation

(2.67). The resulting finite element form of the odd-parity equations is

$$\underline{\bar{X}}^{n}_{1,-1} = \frac{1}{(\Sigma-\Sigma_{s,1})}\left[-\frac{1}{\sqrt{6}}\left(\underline{\underline{\frac{\partial N}{\partial Y}}}\right)\underline{\underline{J}}^{n}\,\underline{\hat{\psi}} + \underline{\underline{J}}^{n}\,\underline{\hat{S}}_{1,-1}\right] \tag{2.97a}$$

and

$$\underline{\bar{X}}^{n}_{1,0} = \frac{1}{(\Sigma-\Sigma_{s,1})}\left[-\frac{1}{\sqrt{3}}\left(\underline{\underline{\frac{\partial N}{\partial X}}}\right)\underline{\underline{J}}^{n}\,\underline{\hat{\psi}} + \underline{\underline{J}}^{n}\,\underline{\hat{S}}_{1,0}\right]. \tag{2.97b}$$

The derivative vectors are denoted as matrices because the term is a matrix with the derivative vector evaluated at node j in row j of the matrix.

A similar procedure is performed to obtain the multigroup sources. For brevity, only the results are presented. The even-parity source equation is

$$\underline{\hat{S}}^{g}_{0,0} = \sum_{n=1}^{NE}\underline{\underline{J}}^{n^{T}}\Bigg[\sum_{g'=1}^{G}\nu\Sigma^{n}_{fg'}\,\underline{\underline{J}}^{n}\,\underline{\hat{\psi}} + \sum_{g'=1}^{g-1}\Sigma^{g'\to g^{n}}_{s,0}\,\underline{\underline{J}}^{n}\,\underline{\hat{\psi}} + \underline{\underline{J}}^{n}\,\underline{\hat{Q}}^{g}_{0,0}\Bigg], \tag{2.98}$$

where

$$\underline{\hat{Q}}^{g}_{0,0} = \sum_{n=1}^{NE}\alpha\;\underline{\underline{J}}^{n^{T}}\;\frac{\int_{\vec{r}_n} d\vec{r}_n\; Q^{g}_{0,0}(X,Y)}{3} \tag{2.99}$$

and

$$\alpha = \begin{cases} 0 \text{ for corner nodes} \\ 1 \text{ for side nodes.} \end{cases}$$

The fixed source, Q, is assumed to be isotropic, therefore, the odd-parity component is zero. The odd-parity sources can now be written as

$$\underline{\hat{S}}^{g}_{1,-1} = \sum_{n=1}^{NE} \underline{\underline{J}}^{n^T} \sum_{g'=1}^{g-1} \Sigma_{s,1}^{g' \to g^n} \underline{\underline{X}}^{n}_{1,-1} \tag{2.100a}$$

and

$$\underline{\hat{S}}^{g}_{1,0} = \sum_{n=1}^{NE} \underline{\underline{J}}^{n^T} \sum_{g'=1}^{g-1} \Sigma_{s,1}^{g' \to g^n} \underline{\underline{X}}^{n}_{1,0} \tag{2.100b}$$

This concludes the derivation of the theoretical model. The following chapter is concerned with the development of the numerical model employed to obtain solutions to Equation (2.94).

CHAPTER III

DEVELOPMENT OF THE NUMERICAL METHOD

This chapter presents the development of the numerical techniques employed in obtaining solutions to the set of coupled algebraic equations that were derived in the previous chapter. The first section of this chapter deals with the numerical integration of the terms in the functional over each element. The iterative strategy and problem termination criteria are discussed in the remaining section.

I. Numerical Integration

The integrals indicated in Equation (2.95) are not simply obtained in closed form. This can be attributed to the higher order approximation used to describe the spatial variation of the flux and the fact that the integrals of the gradient terms depend on the location of the particular element in the mesh. For these reasons, a numerical integration scheme is employed to evaluate the necessary coefficients in the integral matrices.

A nine point quadrature set, Table I[23], is used to perform the integrations over the area of the triangles. The integration points, R_i and S_i, and the weights, w_i, are defined in a transformed coordinate system in which all triangles are mapped as the triangle illustrated in Figure 4. To perform the integrations in the global, X-Y, coordinate system, it is necessary to map the integration

TABLE I

NINE POINT QUADRATURE SET FOR TRIANGLES

R_i	S_i	W_i
0.10271765483	0.80869438567	0.05581442049
0.45570602025	0.45570602025	0.08930307278
0.80869438567	0.10271765483	0.05581442049
0.06655406786	0.52397906774	0.06367808510
0.29526656780	0.29526656780	0.10188493615
0.52397906774	0.06655406786	0.06367808510
0.02303113229	0.18840940591	0.05581442049
0.10617026910	0.10617026910	0.08930307278
0.18840940591	0.02393113229	0.05581442049

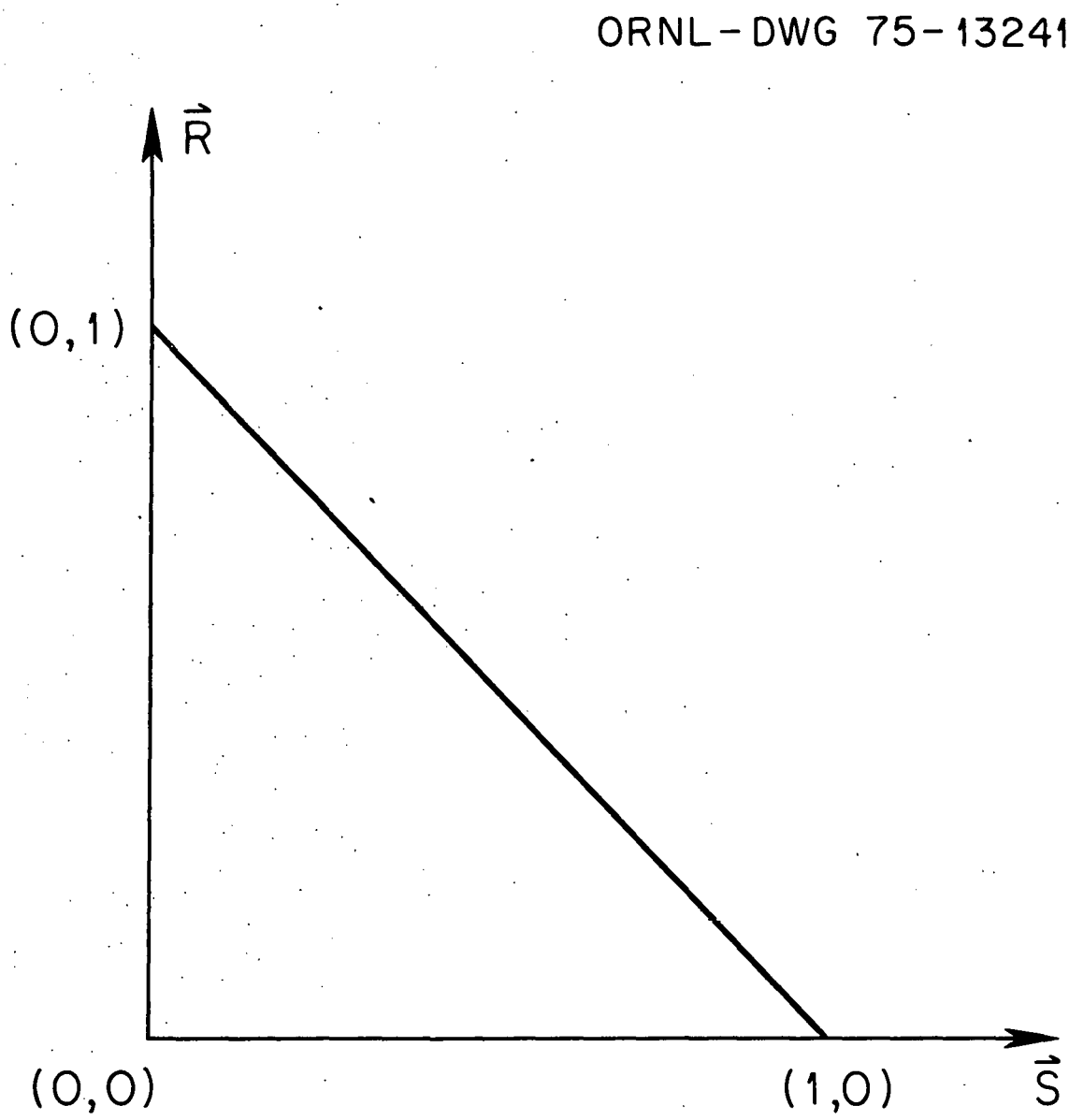

Figure 1. The Triangular Domain in which the Integration Points are Defined.

points into the global system. This is accomplished by envoking the following transformations;

$$\bar{X}_i = (X_3 - X_1)\, R_i + (X_2 - X_1)\, S_i + X_1, \tag{3.1a}$$

$$\bar{Y}_i = (Y_3 - Y_1)\, R_i + (Y_2 - Y_1)\, S_i + Y_1, \tag{3.1b}$$

and

$$\bar{w}_i = 2\, w_i\, \Delta, \tag{3.1c}$$

where X_1, Y_1, X_2, etc. are the coordinates of the corner nodes of the triangle in the global system and Δ is the area of the triangle. The integral of the function of interest, $f(x,y)$, over the triangle is then approximated as

$$\int_{\vec{r}_n} f(X,Y)\, d\vec{r}_n \simeq \sum_{i=1}^{9} f(\bar{X}_i, \bar{Y}_i)\, \bar{w}_i. \tag{3.2}$$

The surface integral for the nonreturn boundary condition is also calculated numerically. A five point Gaussian integration quadrature set is used. The integration points and weights are presented in Table II[24] and are defined on the interval from -1.0 to 1.0. The transformation equations for the surface integral are

$$\bar{X}_i = [(X_2 - X_1)\, R_i + (X_1 + X_2)]/2, \tag{3.3a}$$

$$\bar{Y}_i = [(Y_2 - Y_1)\, R_i + (Y_1 + Y_2)]/2, \tag{3.3b}$$

and

$$\bar{w}_i = w_i[(X_1 - X_2)^2 + (Y_1 - Y_2)^2]^{1/2}/2, \tag{3.3c}$$

TABLE II

FIVE POINT QUADRATURE SET FOR LINES

R_i	w_i
-0.90617985938	0.23692688505
-0.53846931010	0.47862867050
0.0	0.56888888889
0.53846931010	0.47862867050
0.90617985938	0.23692688505

where X_j and Y_j are the coordinates of the end points of the surface to be integrated over. The surface integral is then approximated by

$$\int_{\vec{\Gamma}_n} f(X,Y)\, d\vec{\Gamma}_n \simeq \sum_{i=1}^{5} f(\bar{X}_i, \bar{Y}_i)\, \bar{w}_i. \tag{3.4}$$

II. The Iterative Procedure

This section presents the development of the iterative strategy. The overall procedure consists of inner iterations with optimum overrelaxation on the spatial mesh at each energy group and outer iterations with acceleration for eigenvalue problems.

Inner Iterations

Inner iterations consists of successive recalculation of the flux values at a given energy, given the inscatter, fission, and distributed sources. For a single energy group, the set of algebraic equations derived in the previous chapter can be represented symbolically by the following matrix equation

$$\underline{\underline{M}}\, \underline{\phi} = \underline{S}, \tag{3.5}$$

where M is simply the coefficient matrix obtained from the spatial operators and the boundary conditions, ϕ is the vector of unknown even-parity fluxes for the group being considered, and S is the source vector for that group.

The matrix, M, is now decomposed as follows

$$\underline{\underline{M}} = \underline{\underline{A}} - \underline{\underline{B}}. \tag{3.6}$$

Equation (3.5) is now rewritten as

$$\underline{\underline{A}}\ \underline{\phi} = \underline{S} + \underline{\underline{B}}\ \underline{\phi}. \tag{3.7}$$

If a set of fluxes is available for iteration, n, namely, ϕ_n, then an iterative scheme such as the following could be initiated.

$$\underline{\phi}_{n+1} = \underline{\underline{A}}^{-1}\ \underline{S} + \underline{\underline{A}}^{-1}\ \underline{\underline{B}}\ \underline{\phi}_n. \tag{3.8}$$

This iteration scheme can be slowly converging depending on the magnitude of the eigenvalues of the iteration matrix, A^{-1} B, all of which are less than unity for a convergent process.

Consider Equation (3.8) where the calculation of the new flux values is based only on the values from the previous iteration. The eigenvalues of the iteration matrix contribute to the error in the current value of the flux according to the following equation,

$$\phi_{i,\infty} - \phi_{i,n} = \sum_j c_{i,j}\ \lambda_j^n. \tag{3.9}$$

Therefore, there is a contribution to the error from each error vector having an associated eigenvalue λ_j which depends on the value $c_{i,j}$ and the iteration number. The value of the eigenvalue λ_j depends only on the matrix constants and not the source values. The value of $c_{i,j}$ depends on the initial flux values.[2] As the number of iterations is increased, the largest eigenvalue dominates the rate of error decay. The ratio of two successive values of Equation (3.9) indicates that the error is reduced by a factor of λ each iteration.

$$\frac{\phi_{i,\infty} - \phi_{i,n}}{\phi_{i,\infty} - \phi_{i,n-1}} = \lambda. \tag{3.10}$$

The use of the latest values of the flux as they become available has the effect of accelerating the rate of convergence. The effect is that of squaring the eigenvalues giving the asymptotic behavior[2]

$$\frac{\phi_{i,\infty} - \phi_{i,n}}{\phi_{i,\infty} - \phi_{i,n-1}} = \lambda^2. \tag{3.11}$$

Equation (3.8) becomes

$$\underline{\phi}_{n+1} = \{\underline{\underline{I}} - [\underline{\underline{A}}^{-1} \underline{\underline{B}}]_L\}^{-1} \{\underline{\underline{A}}^{-1} \underline{S} + [\underline{\underline{A}}^{-1} \underline{\underline{B}}]_u \underline{\phi}_n\} \tag{3.12}$$

when the latest values of the flux are used. The matrix I is the identity matrix which is defined elsewhere.[25] This is a significant improvement over simple point relaxation.

The iterative fluxes can also be driven with overrelaxation using the following relationship

$$\phi_{i,n} = \phi_{i,n-1} + \beta_n(\phi^*_{i,n} - \phi_{i,n-1}) \tag{3.13}$$

where $\phi^*_{i,n}$ is the newly calculated flux value and β_n is the overrelaxation coefficient for iteration n. The overrelaxation coefficient can be optimized as follows

$$\beta_{opt} = \frac{2}{1 + \sqrt{1-\alpha}} \tag{3.14}$$

where

$$\alpha = \frac{1}{\lambda}\left[\frac{\lambda+\beta-1}{\beta}\right]^2 \tag{3.15}$$

using the following definitions:

λ is the dominate eigenvalue of the iterative process,

β is the current overrelaxation coefficient, and

$\alpha^{1/2}$ is the spectral radius.

The discussion of acceleration techniques has, to this point, been based on the theory developed for p-cyclic matrices[26] which arise from the finite differencing of elliptic differential equations. To test the applicability of these techniques to the finite element equations, a numerical experiment was performed. Estimates of the dominate eigenvalue were obtained from successive ratios of the L_1 norm which is defined as follows,[2]

$$\lambda_n \simeq \frac{\sum_{i=1}^{NDF} |\phi_{i,n} - \phi_{i,n-1}|}{\sum_{i=1}^{NDF} |\phi_{i,n-1} - \phi_{i,n-2}|}, \tag{3.16}$$

where NDF is the number of space points. The equations were then iterated with a fixed value of β until the dominate eigenvalue was identified. This was done for various values of β.

The results for a one group homogeneous problem are shown in Figure 5. The theory using the calculated value of α predicts that the optimum value of the overrelaxation coefficient should be 1.385. The numerical results confirm that this is the optimum.

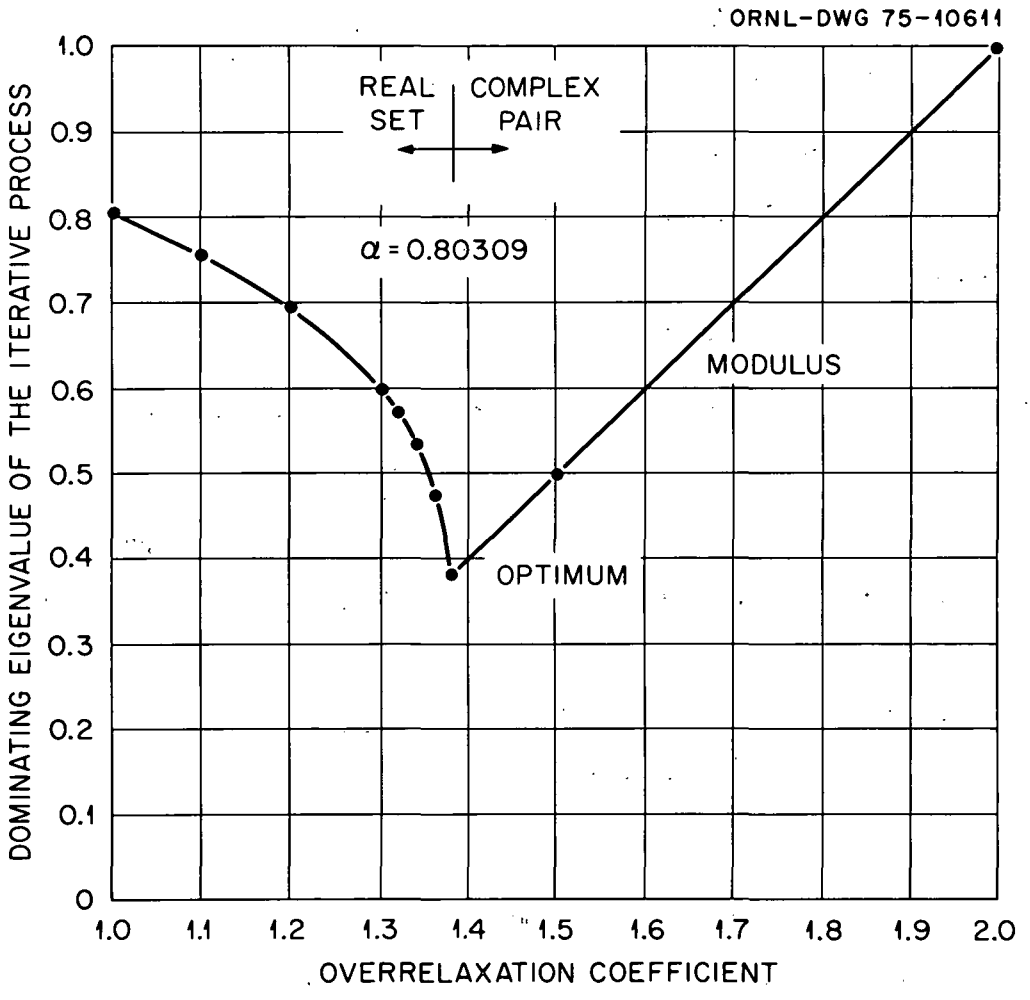

Figure 5. Dependence of the Dominating Eigenvalue on the Overrelaxation Coefficient.

The importance of the use of an overrelaxation coefficient near the optimum is evident from Figure 5. This figure indicates that the error reduction is a factor of 0.38 for each iteration with overrelaxation as compared to 0.80 without overrelaxation. Therefore, for this problem, each iteration performed with the optimum coefficient is equivalent to five iterations done without it.

New values can be obtained for a block of points simultaneously. When this block relaxation method is used, the new values are overrelaxed simultaneously. The block relaxation method is the method used in this work. The overrelaxation coefficients are calculated in the same manner as for the point relaxation method.

The overrelaxation coefficients are also allowed to vary from one energy group to the next. This allows a more efficient use of the procedure by permitting the optimum coefficient to be used in each group.

A further discussion of the matrix splitting and its effect on the convergence of the iterative process is presented in Appendix B.

Outer Iterations

Each outer iteration consists of a full sweep through the energy groups to obtain new estimates of the point flux values. The calculation begins in the first or highest energy group and proceeds downward. For adjoint problems, the sweep is reversed.

The iterative procedure for k eigenvalue problems is relatively simple. The total fission source is calculated after each outer iteration using the following relationship

$$FS_n = \sum_{g=1}^{G} \sum_{i=1}^{NE} \nu\Sigma_{fg,i}\, \phi_{g,i,n}\, \Delta_i. \tag{3.17}$$

The n^{th} estimate of the eigenvalue is then calculated from the following equation

$$k_n = FS_n / FS_{n-1}. \tag{3.18}$$

Once an estimate of the eigenvalue is obtained, the fission source is renormalized and the iterative process if repeated.

The iterative procedure for problems in which there is a fixed source present in a multiplying media is somewhat more complicated. This can be attributed to two effects in particular. First, the presence of the constant source term tends to perturb the solutions approach to an asymptotic distribution. Second, after the convergence to an asymptotic distribution is obtained, each iteration contributes approximately $(k)^n$ Q new fission neutrons. Thus, for problems that are only slightly subcritical, a large number of iterations are required to generate the total fission source. In order to expedite the calculation, an asymptotic extrapolation procedure[2] is employed.

It is assumed that the error in the outer iteration flux vector can be expanded into a set of linearly independent error vectors,

$$\underline{\phi}_{\infty} - \underline{\phi}_{n} = \sum_{j} \left[\prod_{\ell=1}^{n} \mu_{\ell,j} \right] B_{j} + O_{i,n} \qquad (3.19)$$

where $O_{i,n}$ is a residual error, associated with the eigenvalue estimate. which hopefully small and decreasing with increasing n. The B_j is diagonal, constant for each component of ϕ associated with some previous state of the problem, and $\mu_{\ell,j}$ represents the eigenvalues of the error vectors.

The single error mode extrapolation procedure is based on the assumption that one error vector dominates asymptotically,

$$\phi_{i,\infty} - \phi_{i,n} = b_i \mu, \qquad (3.20)$$

where b_i is a constant and μ is the dominating eigenvalue. As in the inner iteration process, estimates of the dominating eigenvalue are obtained from ratios of successive value of the L_1 norm which, for outer iterations, is defined as

$$\mu_n = \frac{\sum_{g=1}^{G} \sum_{i=1}^{NE} |\phi_{g,i,n} - \phi_{g,i,n-1}|}{\sum_{g=1}^{G} \sum_{i=1}^{NE} |\phi_{g,i,n-1} - \phi_{g,i,n-2}|} . \qquad (3.21)$$

Once the iteration procedure stablizes and the dominate eigenvalue is identified, the group fluxes can be extrapolated using

$$\phi_{g,i,\infty} = \phi_{g,i,n} + d(\phi_{g,i,n} - \phi_{g,i,n-1}), \qquad (3.22)$$

where

$$d = \frac{\mu}{1-\mu} \qquad (3.23)$$

and μ is the dominate eigenvalue.

The powerfulness of this method is illustrated by this simple example. The two group problem shown in Figure 6 was calculated with and without asymptotic extrapolations. The fixed source is in the highest energy group and the k eigenvalue is 0.8715. When the extrapolation procedure was not used, 81 outer iterations were required to calculate the total fission source. The use of the extrapolations reduced the number of outer iterations required to reach the same degree of convergence to 10. Clearly, the amount of calculational time saved by using the extrapolations is well worth the minimal effort required to implement the method.

Once a calculation is underway, it is necessary to measure the degree of convergence of the solution. Two quantities are checked to measure convergence. The first is the maximum relative flux change between two successive inner iterations. The second is the fractional deviation of the eigenvalue between two successive outer iterations. When both of these quantities are less than some prespecified value, the problem is considered converged and then terminated.

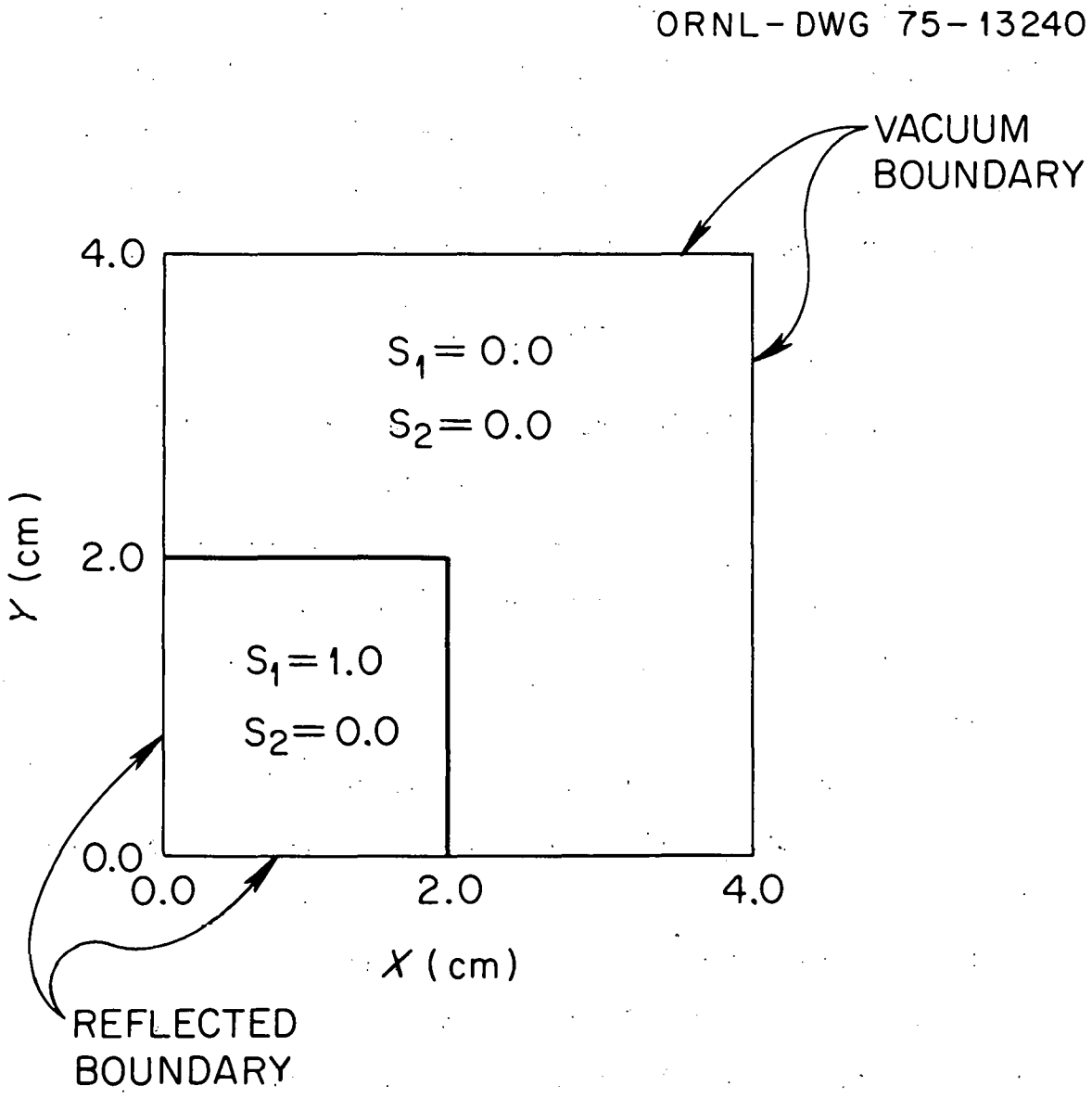

Figure 6. Asymptotic Extrapolation Test Problem Model.

CHAPTER IV

NUMERICAL RESULTS

This chapter presents the results of three numerical experiments. The solutions obtained from the computer code FEP1, which was developed for this dissertation, are compared with the solutions obtained from various established computer codes. All calculations were performed using the IBM 360/91 computer.

I. The Fixed Source Problem

The purpose of this problem is to demonstrate the behavior of the solution method in a scattering material. The calculational model consists of a 6 × 10 cm. rectangle with vacuum boundaries on all four sides. The fixed source is located in the last centimeter along the cm. side. The model is illustrated in Figure 7.

FEP1 and the discrete ordinates transport code DOT III[27] were used to obtain solutions to the problem. The diffusion theory mode was used in DOT III as well as the transport mode. The results of the calculations are shown in Figures 7 and 8.

Figure 7 is a plot of a flux traverse in the X-direction at Y = 2.5 cm. The DOT III diffusion theory solution and the FEP1 solution are in excellent agreement. The S_2 transport solution exhibits nonphysical ripples which are commonly referred to as ray effects and often arise in problems that have low

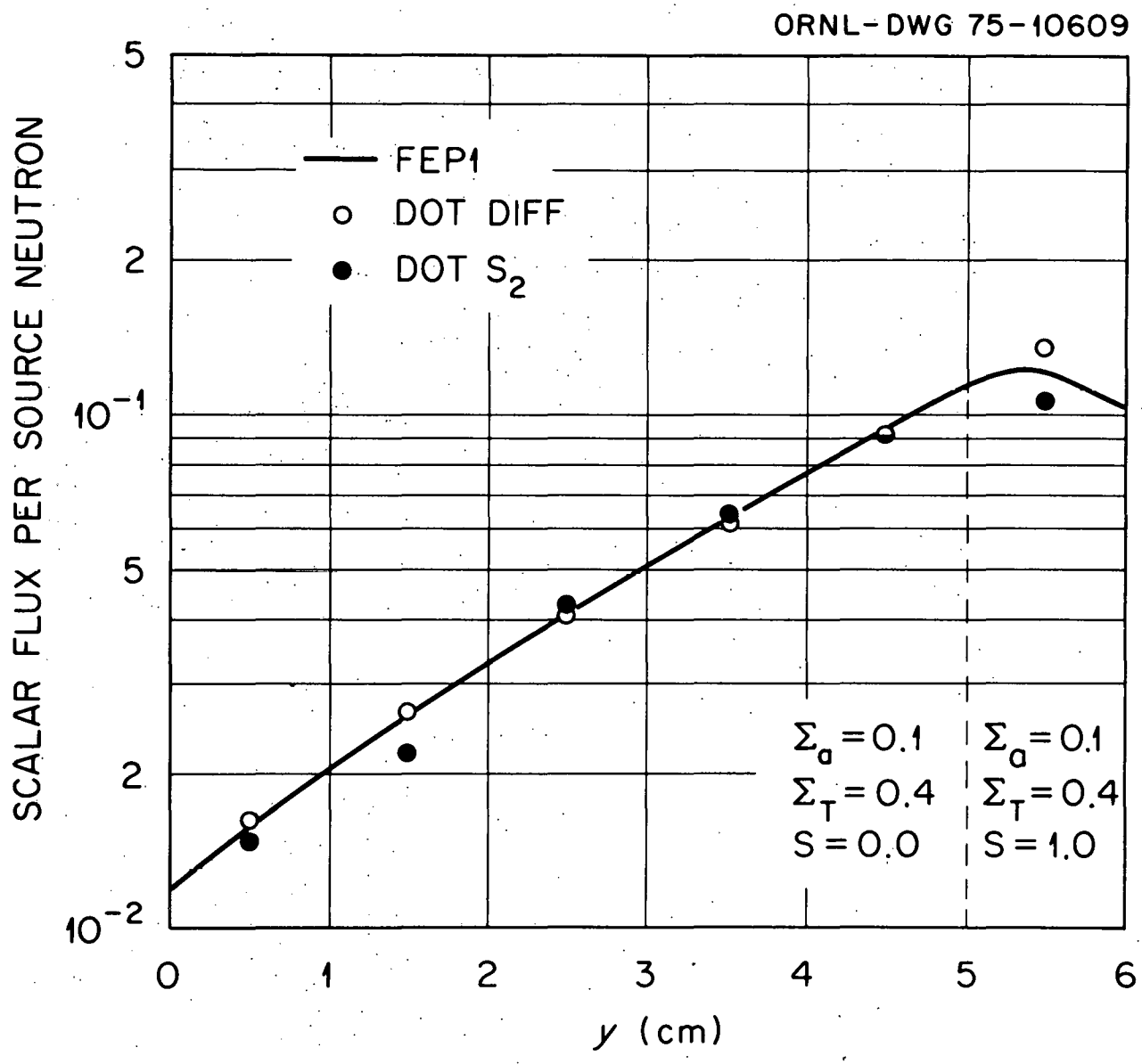

Figure 7. The Fixed Source Problem Model and Flux Traverse at Y=2.5 cm.

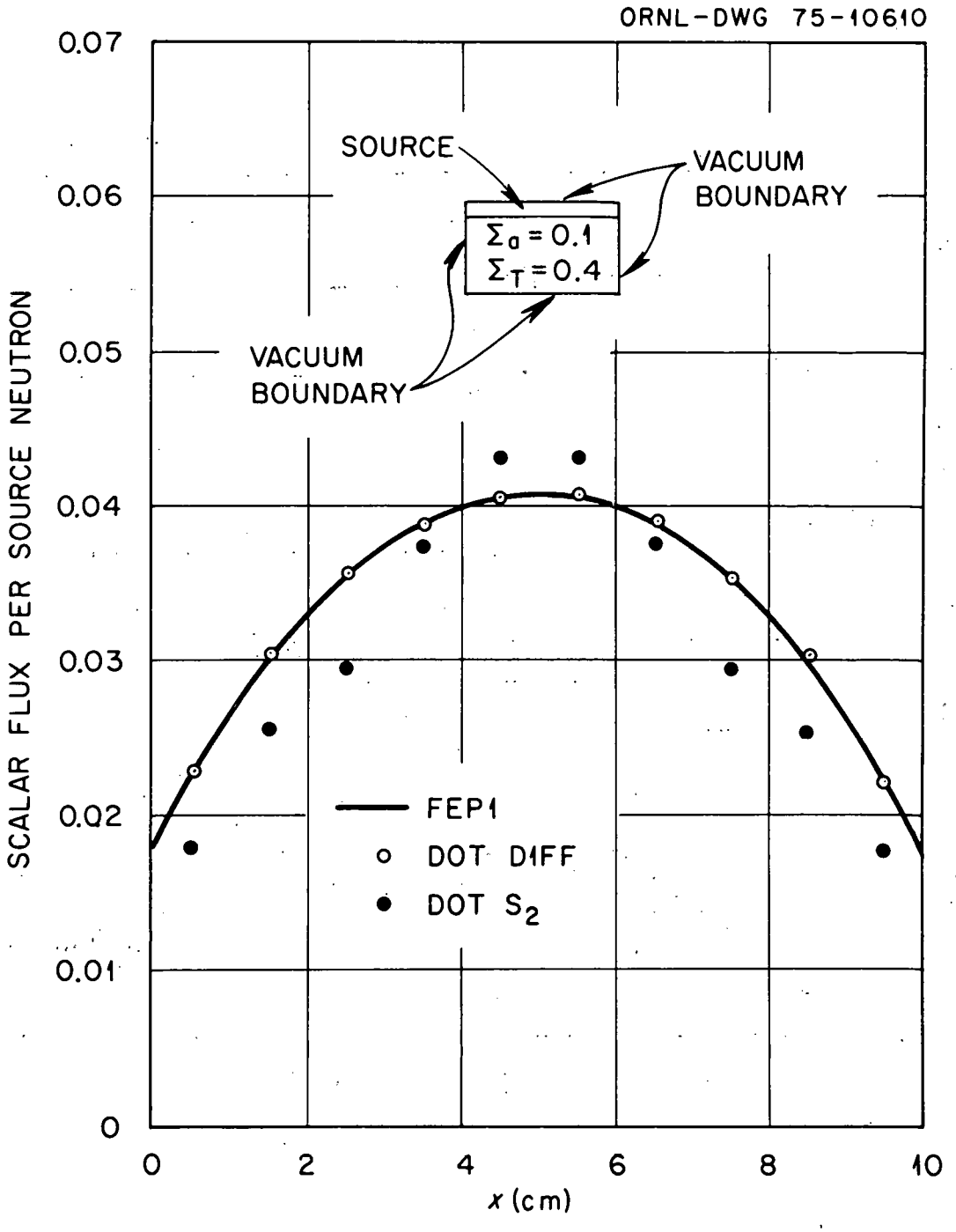

Figure 8. The Fixed Source Problem Flux Traverse at X=5.0 cm.

scattering ratios. Now shown are the S_4 results. The increase in quadrature mitigates these ray effects and then this solution is also in excellent agreement with the FEP1 and diffusion theory results.

Figure 8 is a plot of a flux traverse in the Y-direction a X = 5.0 cm. As before, the FEP1 and diffusion theory solutions are in excellent agreement. The ray effects are apparent in the S_2 solution, but are mitigated by the increase in quadrature to S_4. The overall agreement of the solutions is excellent.

II. The Diffusion Theory Problem

The purpose of this problem is to demonstrate various features of the finite element method that are incorporated in this study. In particular, the ability to calculate k_{eff} eigenvalues for few group problems, the ability to calculate forward and adjoint flux distributions, and the ability to perform these calculations using meshes composed for irregular triangles of various sizes. The capability of using nonorthogonal boundaries is also illustrated.

The problem model suggested by Yang and Henry[28] consists of a highly heterogeneous thermal reactor core, Figure 9. The right and diagonal boundaries are reflected boundaries and the lower boundary is a nonreturn (vacuum) surface. The two group nuclear data is presented in Table III.

A number of calculations were performed using the finite difference diffusion theory computer code VENTURE[2,29] to provide

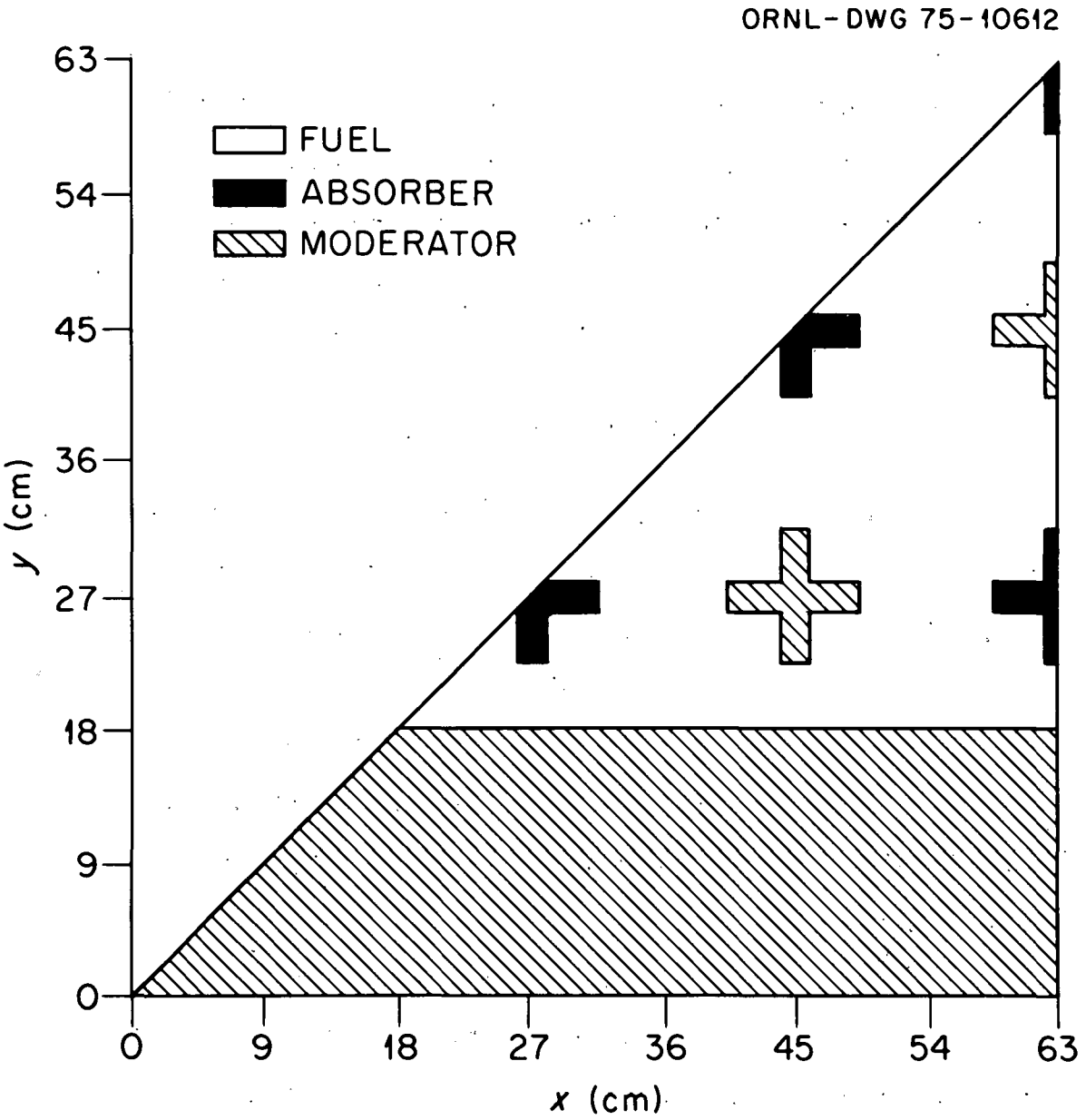

Figure 9. The Diffusion Theory Problem Model.

TABLE III

NUCLEAR DATA FOR THE DIFFUSION THEORY PROBLEM

	Fission Material	Absorber Material	Moderator Material
D_1 (cm)	1.436	1.092	1.545
Σ_1 (cm^{-1})	0.02647	0.003185	0.028824
$\nu\Sigma_{f1}$ (cm^{-1})	0.007293	0.0	0.0
Σ_{21} (cm^{-1})	0.01596	0.0	0.02838
χ^*_1	1.0	0.0	0.0
D_2 (cm)	0.3868	0.3507	0.3126
Σ_2 (cm^{-1})	0.1018	0.4021	0.008736
$\nu\Sigma_{f2}$ (cm^{-1})	0.1531	0.0	0.0
χ_2	0.0	0.0	0.0

*χ refer to the fission spectrum, not the odd-parity flux.

a basis for comparison. Since VENTURE was unable to calculate the nonorthogonal boundary, it was necessary to use a square model of the problem rather than a triangular model. Two calculations were performed using this model. The first was done on a 58 x 58 mesh and the second on a 116 x 116 mesh. The k_{eff} eigenvalues from these calculations are presented in Table IV including the calculation times. The eigenvalue reported for the infinite number of mesh points is an extrapolated value based on the two solutions already discussed.

A single calculation was performed using the FEP1 computer code. The mesh employed in the calculation is shown in Figure 10. Triangles of arbitrary size and orientation were used to illustrate the variety of types of triangles that can be employed in describing the problems geometry. A relatively coarse mesh (337 nodes, 150 triangles) was used to describe the problem. The k_{eff} eigenvalue results for this calculation are also presented in Table IV along with the computation time.

The eigenvalues obtained from both methods are in excellent agreement. The computation time per unknown flux is significantly shorter for the finite difference calculation than it is for the finite element calculation. This is more than offset by the ability of the finite element method to use a coarser mesh and non-orthogonal boundaries making computation times competitive.

The eigenvalue is not the only item of interest in most reactor physics calculations. The forward and adjoint flux

TABLE IV

DIFFUSION THEORY PROBLEM RESULTS

	No. of Nodes	k_{eff}	%Δk	CPU(MINS)
VENTURE (Extrapolated)	∞	1.0398	0.0	---
VENTURE	116 × 116	1.0405	0.067	5.334
VENTURE	58 × 58	1.0426	0.269	1.113
FEP1	337	1.0391	-0.067	0.720

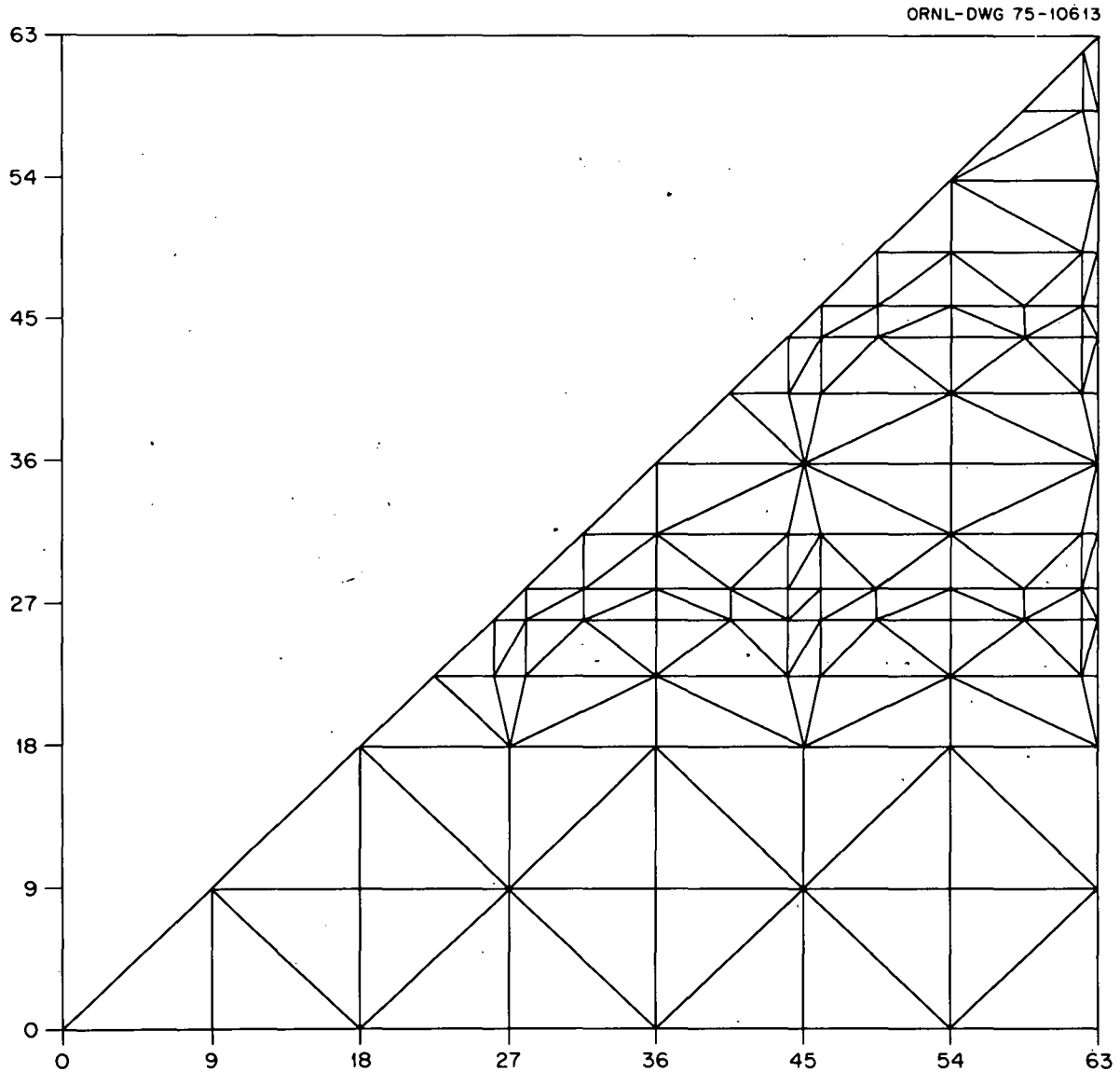

Figure 10. Triangular Mesh for the Diffusion Theory Problem.

distributions are also of interest to analysts. For this reason, a comparison of flux shape is also presented.

A plot of the first and second group scalar fluxes are shown in Figures 11 and 12 respectively. The traverse is in the Y-direction at X = 63.0 cm. The agreement with VENTURE is excellent except near the vacuum boundary. The reason for the discrepancy is the type of boundary condition used in each calculation. The VENTURE calculations used a zero flux boundary condition, i.e., the scalar flux is zero at the boundary, while the FEP1 calculation used a nonreturn boundary condition, i.e., the inward directed partial current is zero.

A plot of the first and second group scalar adjoint fluxes are shown in Figures 13 and 14 respectively. The traverse is at the same section as the forward flux traverse. As before, the agreement with the finite difference solution is excellent.

The results of this problem indicate that the proposed method provide a viable tool for obtaining coarse mesh solutions to the neutron diffusion equations on an irregular triangular mesh with nonorthogonal boundaries.

III. The Transport Theory Problem

The purpose of the third and final test problem is to demonstrate the ability of the proposed method to calculate the k_{eff} eigenvalue and ex-core reaction rates for fast reactor problems in which the effects of linearly anisotropic scattering are important. The model is a modified version of the X-Y model suggested for the FTR (Fast Test Reactor)[30] and is shown in Figure 15.

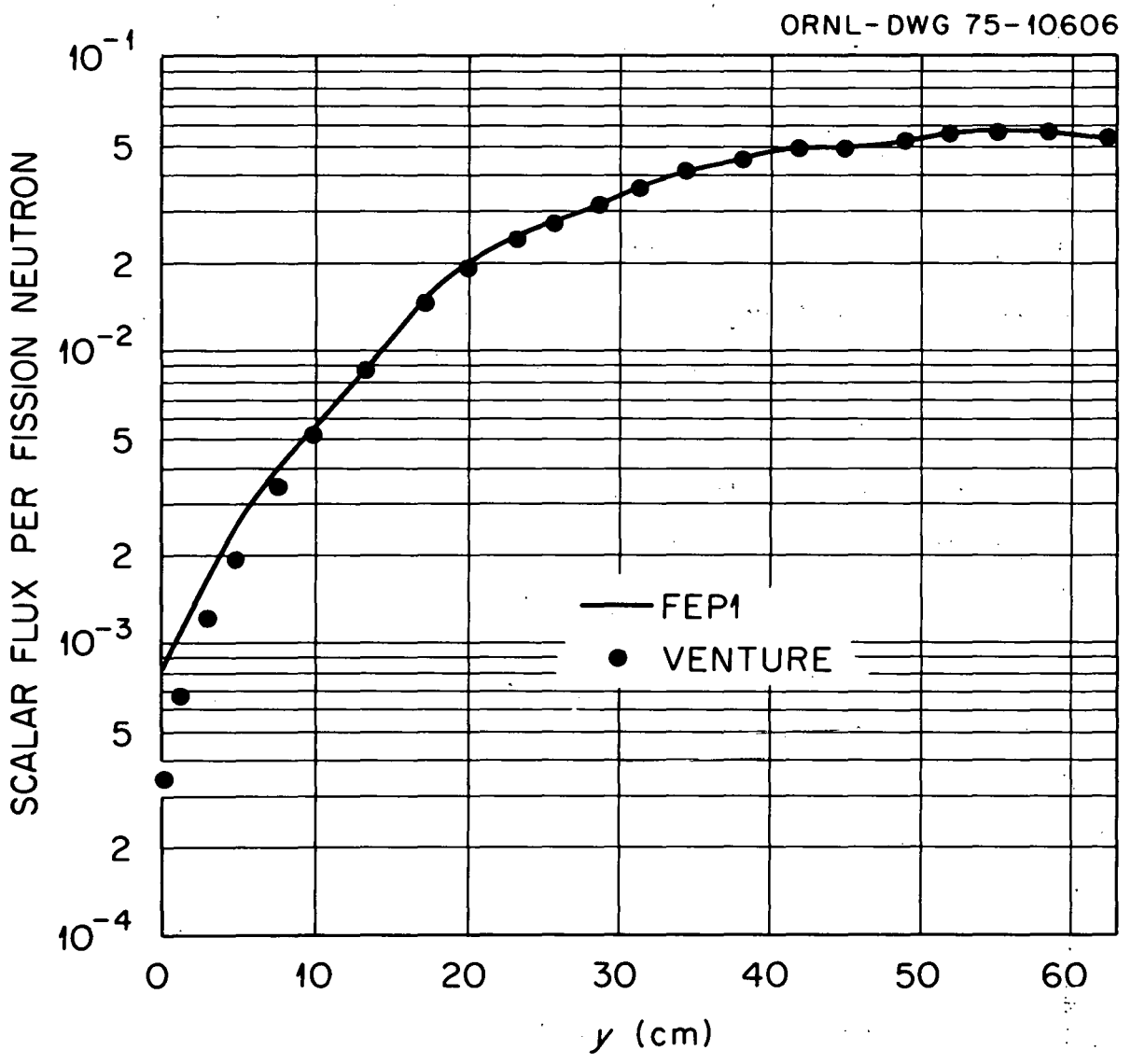

Figure 11. The Diffusion Theory Problem-Group 1 Flux Traverse at X=63.0 cm.

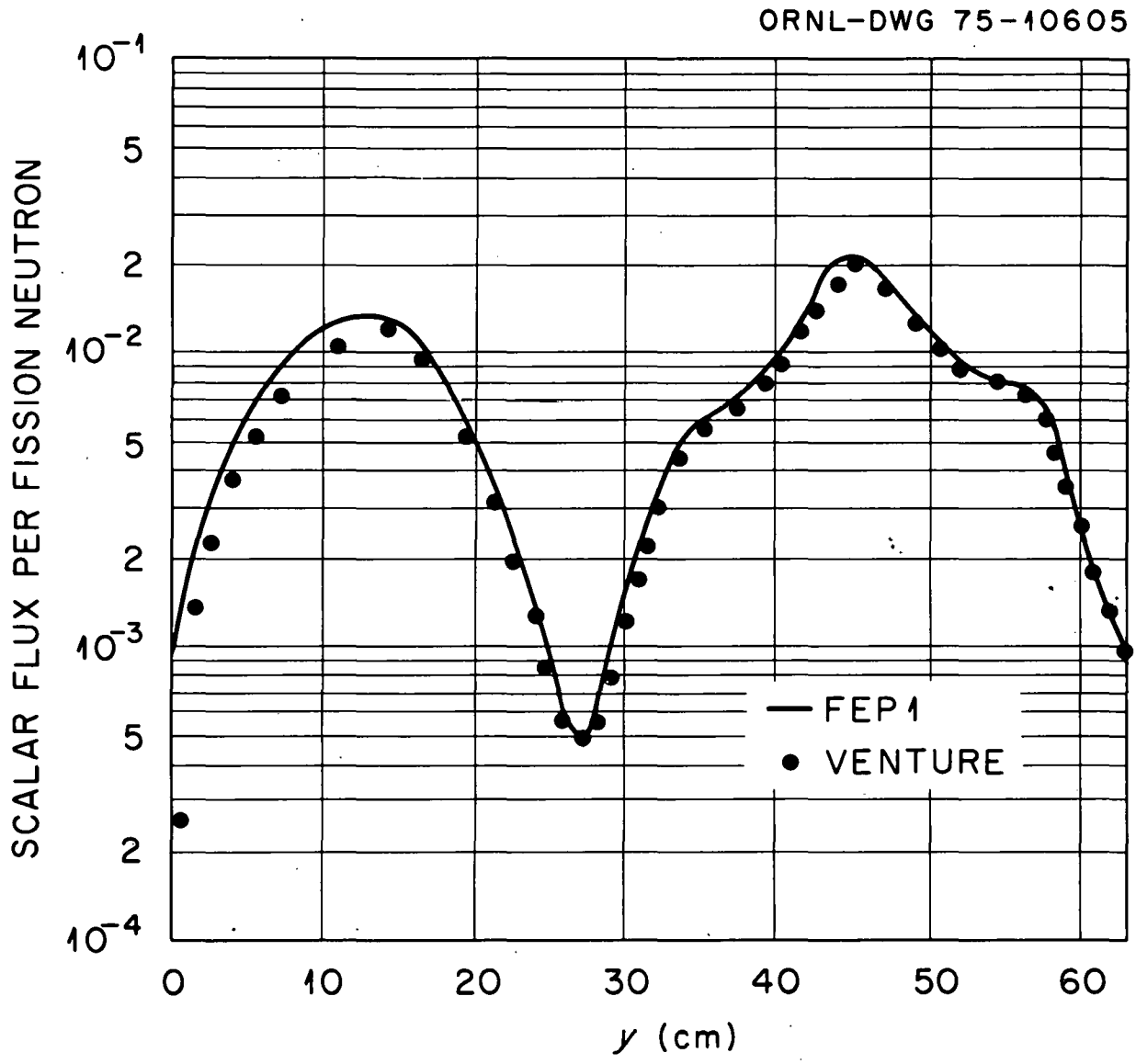

Figure 12. The Diffusion Theory Problem-Group 2 Flux Traverse at X = 63.0 cm.

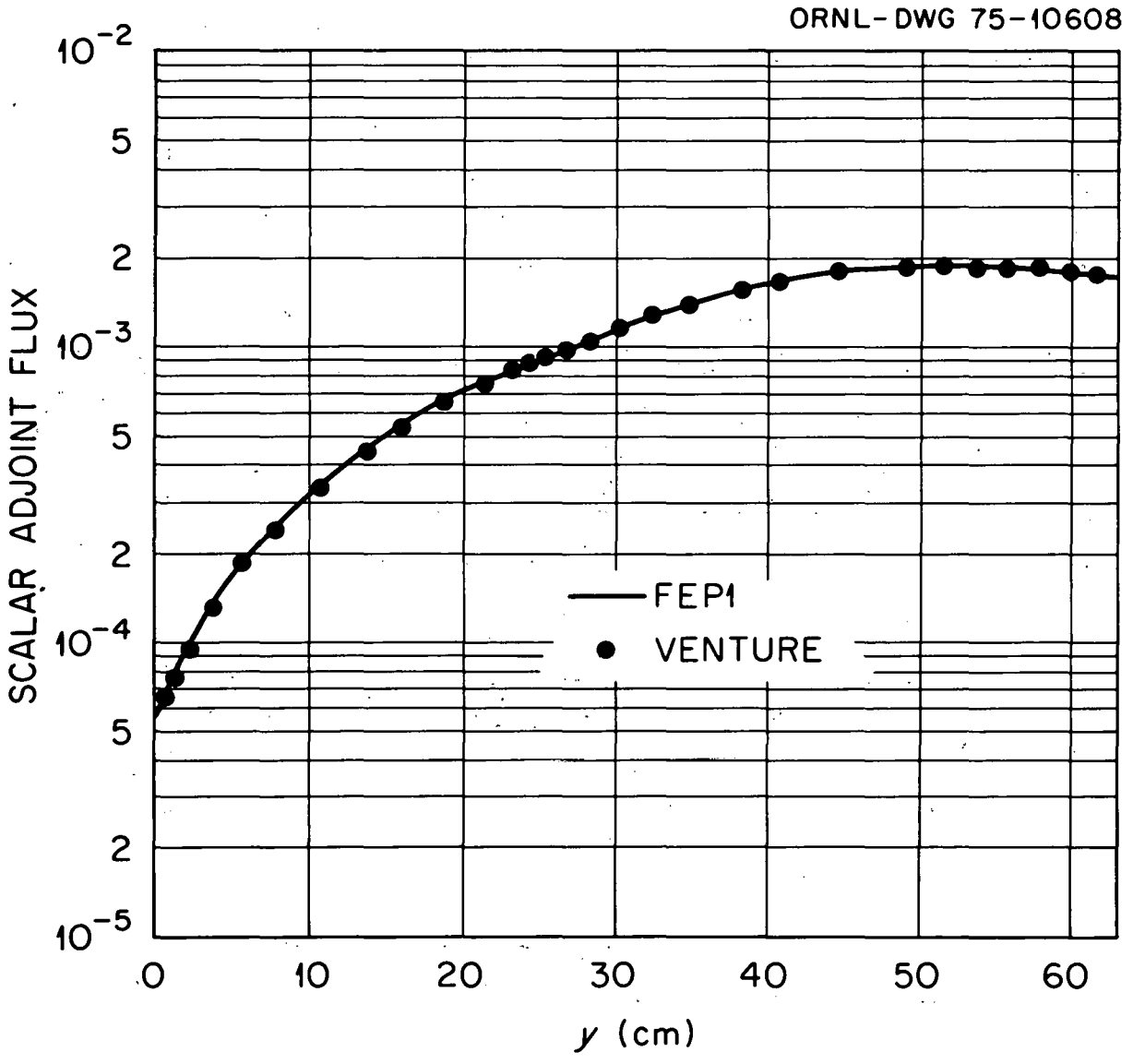

Figure 13. The Diffusion Theory Problem-Group 1 Adjoint Flux Traverse at X=63.0 cm.

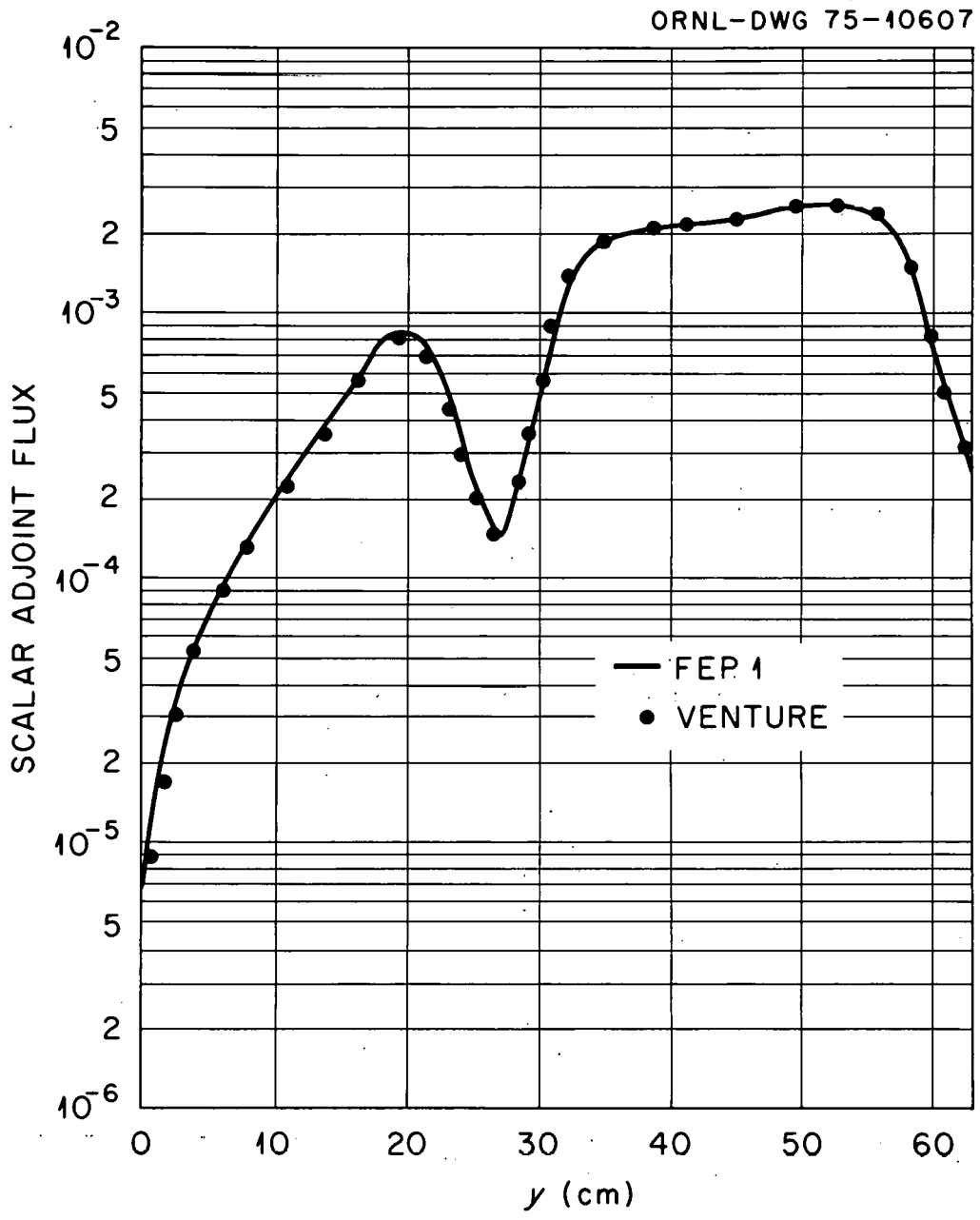

Figure 14. The Diffusion Theory Problem-Group 2 Adjoint Flux Traverse at X=63.0 cm.

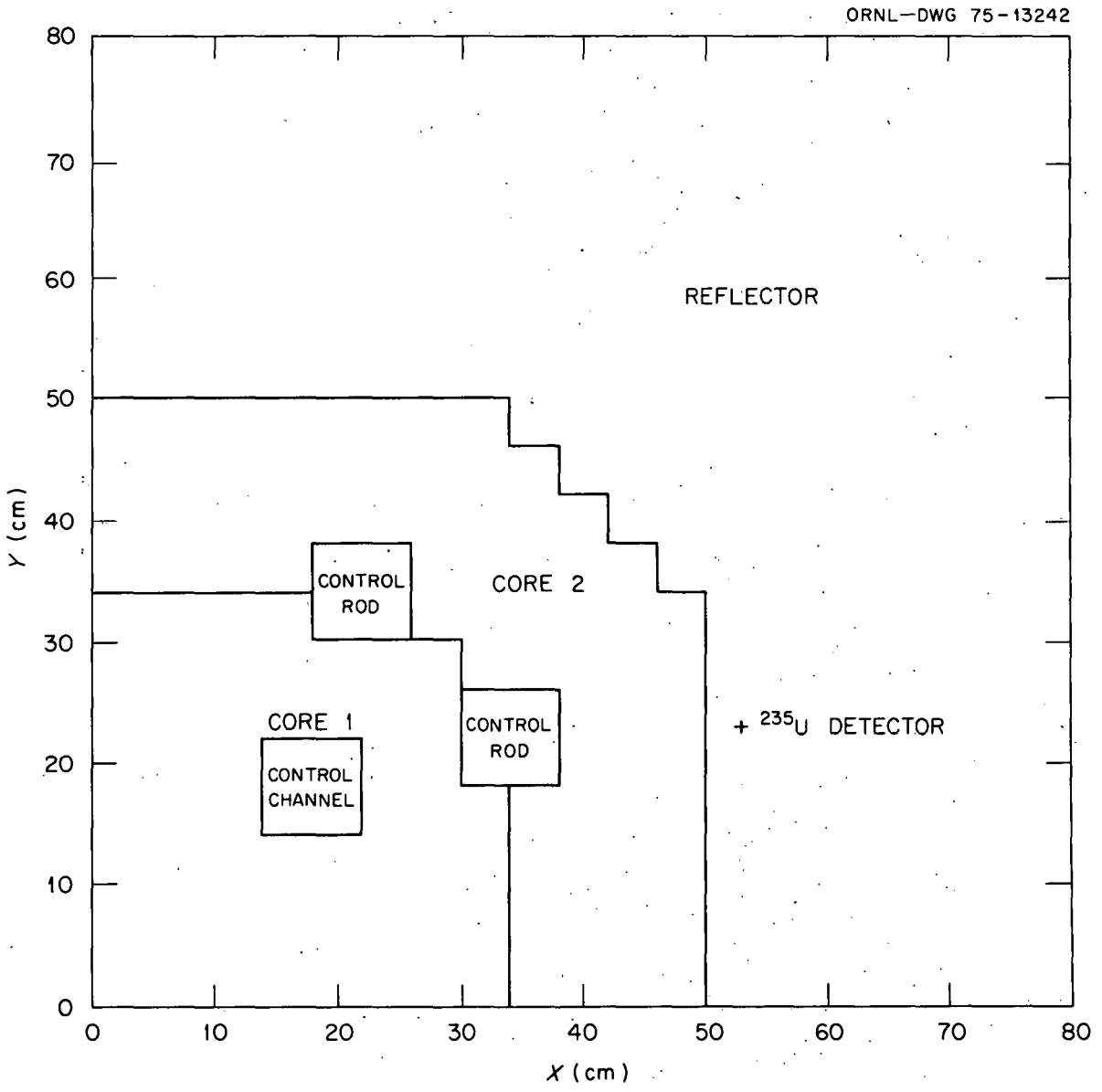

Figure 15. Transport Theory Problem Model.

The original 51 group cross section set with a P_3 expansion of the scattering cross section was produced by the AMPX[31] system. The cross sections were then collapsed to a 7 group set using a one-dimensional model of the problem in the discrete ordinate code ANISN.[32] A transport corrected P_0 set and a P_1 set of cross sections were then produced by the AXMIX[33] code. The transport correction used to modify the total cross section was done using the "inflow approximation" defined by the following equations

$$\Sigma_{TR}(E) = \Sigma(E) - \bar{\mu}_{0,s}(E)\ \Sigma_s(E) \tag{4.1}$$

where

$$\bar{\mu}_{0,s}(E)\ \Sigma_s(E) = \frac{1}{3}\ \frac{\int_E^{\infty} \Sigma_{s,1}(E'\rightarrow E)\ J(E')\ dE'}{J(E)} \tag{4.2}$$

$\Sigma_{TR}(E)$ is the transport cross section, and

$J(E)$ is the neutron current.

A number of calculations were performed to assess the effects of linearly anisotropic scattering. Included in the comparison are the results obtained from the discrete ordinate code DOT3P5,[34] which is an updated version of DOT 111, the Monte Carlo code KENO,[35,36] and the finite element code FEP1. The KENO calculations were performed on the model shown in Figure 15 and followed some 20100 neutron histories. The discrete ordinates and diffusion calculation performed using DOT3P5 were done on a 40 × 40 square mesh. The finite element solution was done on a triangular mesh which included only half the problem model. The triangular mesh consists of 447 nodal points and 201 triangular elements. The

convergence criteria for the two deterministic codes, DOT3P5 and FEP1, was that the maximum fractional deviation in the eigenvalue be less than 10^{-4}. The results of these calculations and the computation times are presented in Table V.

The percent differences in the k eigenvalue are calculated assuming the value obtained from the KENO P_1 calculation is exact. The exclusion of all the anisotropic effects of neutron scattering leads to an error of approximately 2.627 percent in k. The use of a transport corrected cross section set tends to reduce the error, but the exclusion of the linearly anisotropic component of the scattering cross section still results in an error of 0.044 percent in k. The same trends are shown by the DOT3P5 and the FEP1 calculations.

A second comparison can be made between the results obtained from DOT3P5 and FEP1 as they both are deterministic methods. Table VI presents such a comparison. The coarse mesh finite element method used in FEP1* gives results that are in excellent agreement with the results obtained from the finite difference method used in DOT3P5.

A complete reactor analysis is concerned with being able to calculate neutron spectra in ex-core positions as well as in-core positions. The eigenvalue tends to reflect the ability of a method to predict in-core spectra. A good measure of the ability of a

---

*Meshes that are approximately three mean free paths between nodes yield good results.

TABLE V

THE EIGENVALUES FOR THE TRANSPORT THEORY PROBLEM

	k_{eff}	%Δk	CPU (MINS)
KENO P_1	1.12413 ±0.00323	0.0	15.04
KENO P_{TR}*	1.12364 ±0.00362	-0.044	13.28
KENO P_0	1.15366 ±0.00338	2.627	13.77
DOT S_4P_1	1.12241	-0.153	22.40
DOT S_2P_1	1.12409	-0.004	15.81
DOT S_4P_0	1.14782	2.107	23.35
DOT S_2P_0	1.15006	2.307	16.45
DOT P_{TR} DIFFUSION	1.12242	-0.152	2.60
DOT P_0 DIFFUSION	1.14811	2.133	2.65
FEP1 P_1	1.12157	-0.227	5.54
FEP1 P_{TR}	1.12237	-0.156	4.92
FEP1 P_0	1.14788	2.113	5.12

*P_{TR} refers to transport corrected cross sections.

TABLE VI

COMPARISON OF DOT AND FEP1 EIGENVALUES

	FEP1		DOT	%Δk†
P_1	1.12157	S_4	1.12241	-0.07
		S_2	1.12409	-0.224
P_{TR}	1.12237	D*	1.12242	-0.004
P_0	1.14788	S_4	1.14782	0.005
		S_2	1.15006	-0.190
		D	1.14811	-0.020

*D refers to the diffusion theory solution.

†$\%\Delta k = [k_{FEP1} - k_{DOT}]/k_{DOT} \times 100.$

method to accurately calculate ex-core spectra is to calculate a reaction rate just outside the core-reflector interface. Table VII presents the reaction rates calculated at such a position using each of the previously discussed methods. As before, the FEP1 and the DOT3P5 results are in excellent agreement.

This concludes the analysis of the test problem. The next chapter presents the conclusions drawn from this study and some recommendations for future study.

TABLE VII

COMPARISON OF EX-CORE ^{235}U REACTION RATES

	FEP1		DOT	%ΔR.R.*†
P_1	9.7800-2	S_4	9.7638-2	0.166
		S_2	9.7537-2	0.270
P_{TR}	9.7579-2	D	9.8991-2	-1.426
P_0	9.2797-2	S_4	9.2811-2	-0.015
		S_2	9.2613-2	0.199
		D	9.4050-2	-1.332

*R.R. denotes reaction rate.

†$\%\Delta R.R. = [R.R._{FEP1} - R.R._{DOT}]/R.R._{DOT} \times 100.$

CHAPTER V

SUMMARY

I. Conclusions

It has been demonstrated that the finite element method developed and tested in this dissertation is capable of performing a variety of reactor physics calculations using a coarse (relative to finite difference) triangular grids with nonorthogonal boundaries. The method is able to span the gap between diffusion theory and full transport theory while still containing diffusion theory as a viable subset.

The properties of the system matrix generated by the implementation of the finite element method posses properties that allow the convergence acceleration techniques developed for the finite difference form of the multigroup diffusion equations to be utilized and optimized. The application of these acceleration devices make computation times for the FEP1 method competitive with methods already in wide use.

The validity of the solutions were evaluated by comparison of the FEP1 solutions with solutions obtained using various other methods. In all cases, the agreement was excellent.

II. Recommendations

This section presents a few recommendations for future efforts.

1. The further development of the code FEP1 into a production oriented code would necessitate the development and implementation of an automated mesh generator. The calculational capabilities of the code need be extended to include search-type problems and upscatter problems.
2. The extension of the algorithm to accommodate three dimensional problems, either by using three-dimensional finite elements or a finite difference formulation, would greatly enhance the versatility of the method.
3. The implementation of isoparametric elements, either in two or three-dimensional calculations would allow the neutronics problems to be solved on deformed meshes. The coupling of the FEP1 neutronics package, with the deformed mesh capability, to a structural mechanics code, where deformation calculations are routinely done using finite elements, would provide a tool capable of generating valuable information on the interaction of the neutronic and mechanical behavior of reactor cores. In the author's opinion, this is the area of greatest potential for the method.
4. FEP1, as presently written, is I/O (input-output) bound. There are any number of remedies for this problem. Two of particular importance are, first, the reblocking of

the data stored on peripheral data sets and second, the performance of multiple inner iterations on each matrix block while it is resident in core. The use of non-FORTRAN I/O subroutines would also decrease the I/O time. However, they would make the running of the code installation dependent and therefore the benefits gained by their use is questionable.

THIS PAGE

WAS INTENTIONALLY

LEFT BLANK

BIBLIOGRAPHY

THIS PAGE

WAS INTENTIONALLY

LEFT BLANK

BIBLIOGRAPHY

1. Fowler, T. B., D. R. Vondy, and G. W. Cunningham, "Nuclear Reactor Core Analysis Code: CITATION," ORNL-TM-2496, Oak Ridge National Laboratory (July 1969).

2. Vondy, D. R., T. B. Fowler, and G. W. Cunninhgam, "VENTURE: A Code Block for Solving Multigroup Neutronics Problems Applying the Finite-Difference Diffusion-Theory Approximation to Neutron Transport," ORNL-5062, Oak Ridge National Laboratory (October 1975).

3. Protsik, R., E. G. Leff, "Users Manual for DOT2DB: A Two-Dimensional Multigroup Discrete Ordinates Transport/ Diffusion Code with Anisotropic Scattering," GEAP-13537, General Electric Company (September 1969).

4. Flanagan, G. F., N. M. Greene, W. W. Engle, Jr., and E. T. Tomlinson, "Comparison of Transport Approximations for Reactor Physics Calculations in a Fast Reactor," Transactions of the American Nuclear Society, 17: 486-488 (November 1973).

5. Lindeman, A. J., G. A. Leaf, and H. G. Kaper, "A Computational Analysis and Evaluation of the Finite Element Method for a Class of Nuclear Reactor Configurations," Computer Methods in Applied Mechanics and Engineering, 4: 97-117, North-Holland Publishing Company (1974).

6. Kaper, H. G., G. A. Leaf, and A. J. Lindeman, "A Timing Comparison Study for Some High Order Finite Element Approximation Procedures and a Low Order Finite Difference Approximation Procedure for the Solution of the Multigroup Neutron Diffusion Equation," Nuclear Science and Engineering, 49: 27-48 (1972)

7. Zienkiewicz, O. C., The Finite Element Method in Engineering Science, London, England: McGraw-Hill Company (1971).

8. Kang, C. M., and K. F. Hansen, "Finite Element Methods for Space-Time Reactor Analysis," Unpublished Doctoral Dissertation, Massachusetts Institute of Technology, Cambridge (November 1971).

9. Semenza, L. A., E. E. Lewis, and E. C. Rossow, "The Application of the Finite Element Method to the Multigroup Diffusion Equation," Nuclear Science and Engineering, 47: 302-310 (1972).

10. Kaper, H. G., G. K. Leaf, and A. J. Lindeman, "Applications of Finite Element Methods in Reactor Mathematics Numerical Solution of the Neutron Diffusion Equation," ANL-7925, Argonne National Laboratory (February 1972).

11. Miller, W. F., Jr., E. E. Lewis, and E. C. Rossow, "The Application of Phase-Space Finite Elements to the One-Dimensional Neutron Transport Equation," Nuclear Science and Engineering, 51: 148-156 (1973).

12. Miller, W. F., Jr., E. E. Lewis, and E. C. Rossow, "The Application of Phase-Space Elements to the Two-Dimensional Neutron Transport Equation in X-Y Geometry," Nuclear Science and Engineering, 52: 12-22 (1973).

13. Kaper, H. G., G. K. Leaf, and A. J. Lindeman, "Applications of the Finite Element Methods in Reactor Mathematics Numerical Solution of the Neutron Transport Equation," ANL-8126, Argonne National Laboratory (October 1974).

14. Lillie, R. A., "A Linear Triangle Finite Element Formulation for Multigroup Neutron Transport Analysis with Anisotropic Scattering," Doctoral Dissertation, The University of Tennessee, Knoxville (December 1975).

15. Reed, W. H., T. R. Hill, F. W. Brinkley, and K. D. Lathrop, "TRIPLET: A Two-Dimensional, Multigroup, Triangular Mesh, Planar Geometry, Explicit Transport Code," LA-5428-MS, Los Alamos Scientific Laboratory (October 1973).

16. Yuan, Y. C., E. E. Lewis, and W. F. Miller, Jr., "Iterative Solution Methods for Two-Dimensional Finite Element Approximations in Neutron Transport," Proceedings of the Conference on Computational Methods in Nuclear Engineering, Vol. II: 85-101 (April 1975).

17. Weinberg, A. M., and E. P. Wigner, The Physical Theory of Neutron Chain Reactions, Chicago, Illinois: The University of Chicago Press (1958).

18. Kaplan, S., and J. S. Davis, "Canonical and Involutory Transformations of the Variational Problems of Transport Theory," Nuclear Science and Engineering, 28: 166-176 (May 1967).

19. Bell, G. I. and S. Glasstone, Nuclear Reactor Theory, New York, New York, Van Nostrand Reingold Company (1970).

20. Smith, D. R., Variational Methods in Optimization, Englewood Cliffs, New Jersey, Prentice-Hall, Inc. (1974).

21. Morse, P. M. and H. Feshback, Methods of Theoretical Physics, New York, New York, McGraw-Hill Company (1953).

22. Kaplan, S., "Variational Methods in Nuclear Engineering," Advances in Nuclear Science and Technology, Vol. 5: 185-207 (1969).

23. Akin, J. E., and W. T. C. Stoddart, "Computer Codes for Implementing the Finite Element Method," Report 75-1, The University of Tennessee (April 1975).

24. Conte, S. D., Elementary Numerical Analysis, New York, New York, McGraw-Hill Company (1965).

25. Noble, B., Applied Linear Algebra, Englewood Cliffs, New Jersey, Prentice-Hall, Inc. (1969).

26. Varga, R. S., Matrix Iterative Analysis, Englewood Cliffs, New Jersey, Prentice-Hall, Inc. (1962).

27. Rhoades, W. A. and F. R. Mynatt, "The DOT III Two-Dimensional Discrete Ordinates Transport Code," ORNL-TM-4280, Oak Ridge National Laboratory (September 1973).

28. Yang, S. and A. F. Henry, "A Finite Element Synthesis Method," Nuclear Science and Engineering (to be published).

29. Vondy, D. R., Oak Ridge National Laboratory, Oak Ridge, Tennessee, personal communication (June 1975).

30. Ramchandran, S., G. J. Calamai, F. J. Baloh, and S. A. Schellin, "Fuel Pin Enrichment Specifications for FTR Cores 1 and 2," WARD-2171-26, Westinghouse Advanced Reactors Division (January 1973).

31. Greene, N. M., J. L. Lucius, L. M. Petrie, W. E. Ford, III, J. E. White, and R. Q. Wright, "AMPX: A Modular Code System for Generating Coupled Multigroup Neutron-Gamma Libraries from ENDF/B," ORNL-TM-3706, Oak Ridge National Laboratory (November 1974).

32. Engle, W. W., Jr., "A User's Manual for ANISN, A One-Dimensional Discrete Ordinates Transport Code with Anisotropic Scattering," ORGDP-K-1693, Oak Ridge Gaseous Diffusion Plant (March 1967).

33. Haynes, G. C., "The AXMIX Program for Cross Section Mixing and Library Arrangement," ORNL Central Files Report 74-12-2, Oak Ridge National Laboratory (December 1974).

34. Simpson, D. B., and W. A. Rhoades, Oak Ridge National Laboratory, Oak Ridge, Tennessee, personal communication (October 1974).

35. Whitesides, G. E., and N. F. Cross, "KENO: A Multigroup Monte Carlo Criticality Program", CTC-5 Union Carbide Corporation-Nuclear Division, Computing Technology Center (September 1969).

36. Fox, P. B., Union Carbide Corporation-Nuclear Division, Oak Ridge, Tennessee, personal communication (September 1975).

APPENDIXES

THIS PAGE

WAS INTENTIONALLY

LEFT BLANK

APPENDIX A

THE ADJOINT PROBLEM

This appendix presents a brief derivation and discussion of the adjoint form of the even-parity functional.

The adjoint form of the Boltzmann neutron transport equation is

$$-\vec{\Omega}\cdot\vec{\nabla}\ \phi^*(X,Y,E,\vec{\Omega}) + \Sigma(X,Y,E)\ \phi^*(X,Y,E,\vec{\Omega}) =$$

$$\int_{E'}\int_{\vec{\Omega}'} \Sigma_s(X,Y,\vec{E}\vec{\Omega}\rightarrow E',\vec{\Omega}')\ \phi^*(X,Y,E,\vec{\Omega}')\ d\vec{\Omega}'dE' +$$

$$\frac{\nu\Sigma_f(E)}{4\pi}\int_{E'}\int_{\vec{\Omega}'} f(E')\ \phi^*(X,Y,E',\vec{\Omega}')\ d\vec{\Omega}'dE' + Q^*(X,Y,E,\vec{\Omega}) \qquad (A.1)$$

where ϕ^* and Q^* are the adjoint flux and adjoint source respectively. The remaining terms are defined in Chapter II, page 9.

The monoenergetic form of the adjoint equation can be written as follows for $\vec{\Omega}$,

$$-\vec{\Omega}\cdot\vec{\nabla}\ \phi^*(\vec{\Omega}) + \Sigma\ \phi^*(\vec{\Omega}) = \int_{\vec{\Omega}'} \Sigma_s(\vec{\Omega}'\cdot\vec{\Omega})\ \phi^*(\vec{\Omega}')\ d\vec{\Omega}' + Q^*(\vec{\Omega}), \qquad (A.2)$$

and for $-\vec{\Omega}$,

$$\vec{\Omega}\cdot\vec{\nabla}\ \phi^*(-\vec{\Omega}) + \Sigma\ \phi^*(-\vec{\Omega}) = \int_{\vec{\Omega}'} \Sigma_s(\vec{\Omega}'\cdot-\vec{\Omega})\ \phi^*(\vec{\Omega}')\ d\vec{\Omega}' + Q^*(-\vec{\Omega}). \qquad (A.3)$$

The adjoint flux is then decomposed as follows

$$\phi^*(\vec{\Omega}) = \psi^*(\vec{\Omega}) - \chi^*(\vec{\Omega}) \tag{A.4}$$

where

$$\psi^*(\vec{\Omega}) = \frac{1}{2}[\phi^*(\vec{\Omega}) + \phi^*(-\vec{\Omega})] \tag{A.5}$$

$$\chi^*(\vec{\Omega}) = \frac{1}{2}[\phi^*(-\vec{\Omega}) - \phi^*(\vec{\Omega})]. \tag{A.6}$$

Using the definitions presented in Chapter II, page 12, for the even and odd-parity parameters allows the canonical form of the adjoint transport equation to be written as

$$\vec{\Omega}\cdot\vec{\nabla}\ \chi^*(\vec{\Omega}) + \Sigma\psi^*(\vec{\Omega}) = \int_{\vec{\Omega}'} \Sigma_s^e(\vec{\Omega}'\cdot\vec{\Omega})\ \psi^*(\vec{\Omega}')\ d\vec{\Omega}' + S^{e*}(\vec{\Omega}) \tag{A.7}$$

and

$$\vec{\Omega}\cdot\vec{\nabla}\ \psi^*(\vec{\Omega}) + \Sigma\chi^*(\vec{\Omega}) = \int_{\vec{\Omega}'} \Sigma_s^o(\vec{\Omega}'\cdot\vec{\Omega})\ \chi^*(\vec{\Omega}')\ d\vec{\Omega}' + S^{o*}(\vec{\Omega}). \tag{A.8}$$

The odd-parity adjoint flux can now be obtained from Equation (A.8).

$$\chi^*(\vec{\Omega}) = \frac{S^{o*}(\vec{\Omega}) - \vec{\Omega}\cdot\vec{\nabla}\ \psi^*(\vec{\Omega})}{\Sigma} +$$

$$\frac{1}{\Sigma}\sum_{\ell_{odd}} \frac{\Sigma_{s,\ell}}{\Sigma-\Sigma_{s,\ell}} \sum_{m=-\ell}^{\ell} Y_{\ell,m}(\vec{\Omega}) \int_{\vec{\Omega}'} Y^+_{\ell,m}(\vec{\Omega}') \times$$

$$[S^o(\vec{\Omega}') - \vec{\Omega}'\cdot\vec{\nabla}\ \psi^*(\vec{\Omega}')]\ d\vec{\Omega}'. \tag{A.9}$$

Equation (A.9) is now substituted into Equation (A.7) to give the even-parity form of the adjoint transport equation

$$\frac{\vec{\Omega}\cdot\vec{\nabla}(\vec{\Omega}\cdot\vec{\nabla})\ \psi^*(\vec{\Omega})}{\Sigma} - \frac{\vec{\Omega}\cdot\vec{\nabla}\ S^{o*}(\vec{\Omega})}{\Sigma} -$$

$$\frac{-\vec{\Omega}\cdot\vec{\nabla}}{\Sigma} \sum_{\ell_{odd}} \frac{\Sigma_{s,\ell}}{\Sigma-\Sigma_{s,\ell}} \sum_{m=-\ell}^{\ell} Y_{\ell,m}(\vec{\Omega}) \cdot$$

$$\{\int_{\vec{\Omega}'} Y^+_{\ell,m}(\vec{\Omega}')[S^{o*}(\vec{\Omega}') - \vec{\Omega}'\cdot\vec{\nabla}\ \psi^*(\vec{\Omega}')]d\vec{\Omega}' +$$

$$\sum_{\ell_{even}} \Sigma_{s,\ell} \sum_{m=-\ell}^{\ell} Y_{\ell,m}(\vec{\Omega}) \int_{\vec{\Omega}'} Y^+_{\ell,m}(\vec{\Omega}')\ \psi^*(\vec{\Omega}')\ d\vec{\Omega}' +$$

$$\Sigma\psi^*(\vec{\Omega}) + S^{e*}(\vec{\Omega}) = 0. \qquad \text{(A.10)}$$

The even-parity functional for the adjoint problem can now be written as follows.

$$F(\psi^*) = \frac{1}{2}\int_{\vec{r}}\int_{\vec{\Omega}} \{\frac{[\vec{\Omega}\cdot\vec{\nabla}\psi^*(\vec{\Omega})]^2}{\Sigma} + \Sigma\psi^*(\vec{\Omega})^2 -$$

$$\psi^*(\vec{\Omega}) \sum_{\ell_{even}} \Sigma_{s,\ell} \sum_{m=-\ell}^{\ell} Y_{\ell,m}(\vec{\Omega}) \int_{\vec{\Omega}'} Y^+_{\ell,m}(\vec{\Omega}')\ \psi^*(\vec{\Omega}')\ d\vec{\Omega}' +$$

$$\vec{\Omega}\cdot\vec{\nabla}\psi^*(\vec{\Omega}) \int_{\vec{\Omega}'} g(\vec{\Omega}'\cdot\vec{\Omega})\ \vec{\Omega}'\cdot\vec{\nabla}\psi^*(\vec{\Omega}')\ d\vec{\Omega}' - \frac{2\vec{\Omega}\cdot\vec{\nabla}\psi^*(\vec{\Omega})\ S^{o*}(\vec{\Omega})}{\Sigma} -$$

$$2\psi^*(\vec{\Omega})\ S^{e*}(\vec{\Omega}) - 2\vec{\Omega}\cdot\vec{\nabla}\psi^*(\vec{\Omega}) \int_{\vec{\Omega}} g(\vec{\Omega}'\cdot\vec{\Omega})\ S^{o*}(\vec{\Omega}')\ d\vec{\Omega}'\}\ d\vec{\Omega}d\vec{r} +$$

$$\frac{\gamma}{2}\int_{\vec{\Gamma}}\int_{\vec{\Omega}} |\vec{\Omega}\cdot\vec{n}|\ \psi^*(\vec{\Omega})^2\ d\vec{\Omega}d\vec{\Gamma} \qquad \text{(A.11)}$$

where $g(\vec{\Omega}'\cdot\vec{\Omega})$ is defined by Equation (2.41).

The form of the adjoint odd-parity flux, Equation (A.9), is the same as the equation for the forward odd-parity flux, Equation (2.33). The same is true for the adjoint functional, Equation (A.11), and the forward functional, Equation (2.54). Therefore, the only change in the computer code needed to perform adjoint calculations is to correctly define the adjoint scattering matrices and the adjoint fission source. If the angular adjoint flux is to be reconstructed, the difference of the even and odd-parity fluxes is required rather than the sum of the fluxes which is required for reconstruction of the forward angular flux.

APPENDIX B

CONVERGENCE

This appendix presents a brief discussion of the convergence behavior of the inner iteration process as a function of the manner in which the system matrix is split.

The splitting used in Chapter III, page 46, is essentially of the following form:

$$\underline{\underline{M}} = \underline{\underline{A}} - \underline{\underline{B}}_U - \underline{\underline{B}}_L , \tag{B.1}$$

where A consists of square blocks along the diagonal and $\underline{\underline{B}}_U$ and $\underline{\underline{B}}_L$ are of the form shown in Figure 16.

According to Varga,[26] Theorem 3.6, Corallary 2, if M is a Hermitian matrix partition as shown in Equation (B.1), and A is positive definite, then the block successive overrelaxation method is convergent for all initial conditions if and only if the over-relaxation coefficient, β, has values between zero and two and M is positive definite.

An investigation of the system matrix for this work reveals that, since the set of algebraic equations was obtained through the variational finite element formulation, the system matrix is guaranteed to be symmetric. The variables in the functional are all real valued, therefore, the elements of the system matrix are also real valued.

ORNL-DWG 75-13239

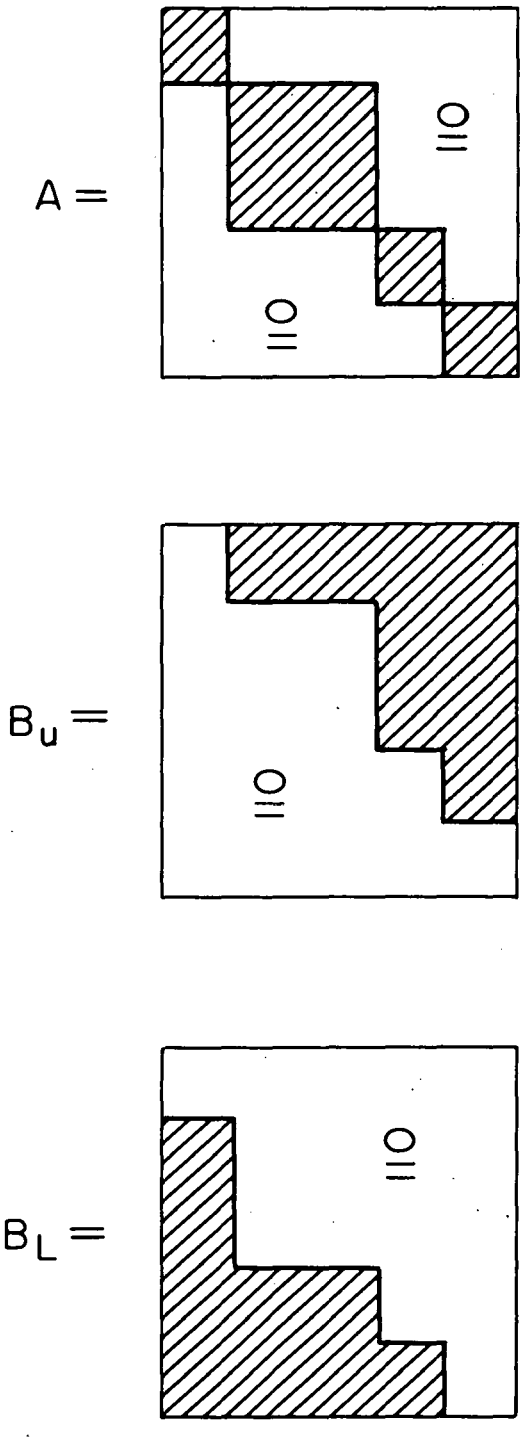

Figure 16. Typical Matrix Splitting.

Further investigation shows that the system matrix is also positive definite. This is because the functional is a quadratic functional and therefore positive definite.

For this work, the value of the overrelaxation coefficient is limited to vary between one and two.

Incorporating these facts concerning the problem of interest with Theorem 3.6, it can be shown that the inner iteration process is convergent as long as the matrix A is chosen to be positive definite.

A number of numerical tests were performed to show the applicability of this proof. It was found that these represent sufficient, but not necessary conditions for convergence.

THIS PAGE

WAS INTENTIONALLY

LEFT BLANK

ORNL/TM-5224
UC-79d - LMFBR Physics

INTERNAL DISTRIBUTION

1-3. L. S. Abbott
4. J. W. Allen
5. R. G. Alsmiller
6. J. D. Amburgey
7. J. Barish
8. D. E. Bartine
9. V. C. Baker
10. J. A. Bucholz
11. T. J. Burns
12. R. L. Childs
13. C. E. Clifford
14. S. N. Cramer
15. N. F. Cross
16. G. W. Cunningham
17. J. D. Drischler
18. M. B. Emmett
19. W. W. Engle, Jr.
20. G. F. Flanagan
21. W. E. Ford
22. V. M. Forsberg
23. T. B. Fowler
24. T. A. Gabriel
25. N. M. Greene
26. W. O. Harms
27. T. J. Hoffman
28. J. D. Jenkins
29. T. W. Kerlin
30. R. A. Lillie
31. J. L. Lucius
32. J. W. McAdoo
33. F. C. Maienschein
34. J. T. Mihalczo
35. J. E. Mott
36. F. R. Mynatt
37. E. M. Oblow
38. Y. M. Ozal
39. J. V. Pace
40. A. M. Perry
41. L. M. Petrie
42. H. Postma
43. K. R. Piety
44. W. A. Rhoades
45-49. J. C. Robinson
50. R. T. Santoro
51. R. W. Roussin
52. D. L. Selby
53. F. S. Shahrokhi
54. D. B. Simpson
55. C. O. Slater
56. P. N. Stevens
57. J. S. Tang
58. M. L. Tobias
59-68. E. T. Tomlinson
69. D. L. Trauger
70. K. R. Turnbull
71. D. R. Vondy
72. C. R. Weisbin
73. R. M. Westfall
74. J. E. White
75. G. E. Whitesides
76. L. R. Williams
77. M. L. Williams
78. R. Q. Wright
79. A. Zucker
80. P. F. Fox (consultant)
81. W. W. Havens (consultant)
82. A. F. Henry (consultant)
83. R. E. Uhrig (consultant)
84-85. Central Research Library
86. Y-12 Document Reference Section
87-88. Laboratory Records Department
89. Laboratory Records, ORNL RC
90-94. RSIC
95. H. Goldstein (consultant)
96. M. L. Tobias

EXTERNAL DISTRIBUTION

97-98. Director, Division of Reactor Research and Development, ERDA, Washington, DC 20545
99. Research and Technical Support Division, ERDA-ORO
100. Director, Reactor Division, ERDA-ORO
101-304. For distribution as shown in TID-4500, Distribution Category, UC-79d, Liquid Metal Fast Breeder Reactor Physics

☆ U.S. GOVERNMENT PRINTING OFFICE: 1976-748-189/233